Complex behavior of a PEO-b-PCL block copolymer in water-ethanol solvent mixtures

Chi, Meng

Award date:
2018

Technische Universiteit Eindhoven University of Technology

Where innovation starts

Department of Chemical Engineering and Chemistry

Laboratory of Physical Chemistry (SPC)

Complex behavior of a PEO-b-PCL block copolymer in water-ethanol solvent mixtures

Master Thesis of

Meng Chi

Supervisors:

Dr. A. C. C. Esteves

MSc. A. Ianiro

Prof. dr. ir. R. Tuinier

Dr. H. Friedrich

SPC Laboratory of Physical Chemistry

Eindhoven, March 2018

Abstract

Block copolymers show high potential for applications in the medical field, namely in drug delivery systems, due to their self-assembly behavior and interfacial properties. In this work, we have explored the possibility of inducing the self-assembly of a stimuli-responsive block-copolymer, poly(ethylene oxide)-block-poly-caprolactone (PEO-b-PCL), in water-ethanol solvent mixtures by tuning the solvency conditions and temperature. In pure ethanol, due to the poor solvent selectivity, PEO-b-PCL loses the ability to self-assemble and undergoes a macro-phase separation, followed by a nano-phase separation upon lowering the temperature. However, with the addition of water, self-assembled vesicle and cylinder structures were induced in solvent mixtures with 20 and 30% water. Under the solvent conditions of pure ethanol and 50% water-ethanol mixtures and using temperature as a control parameter, nanoscale assemblies of body-centered-cubic (BCC) and face-centered-cubic (FCC) morphologies were observed by SAXS performed below the cloud points, respectively. Inside these nano-phase separated domains crystallization of the polymer blocks also occurs. While both blocks crystallize in ethanol, the addition of water hindered the crystallization of PEO block.

Key words: self-assembly, phase separation, PEO-b-PCL, thermoresponsive, solvent composition

Contents

Block copolymers are a particular class of copolymers composed by two or more blocks that allows them to self-assemble in solution into different supramolecular structures. These structures can be used, for example, as in vivo drug delivery systems. Poly(ethylene oxide)-block-poly-caprolactone (PEO-b-PCL) block copolymers are ideal for these applications due to their biocompatibility and biodegradability.

The preparation of these self-assembled structures often involves the use of toxic organic solvents, therefore it is crucial to develop more biocompatible routes to prepare and manipulate such structures. Water-ethanol mixtures represent an interesting alternative to classic organic solvents due to their low toxicity and peculiar “non-ideal” properties.

The aim of this project is therefore to explore the behavior of PEO-b-PCL copolymer in water ethanol mixtures, focusing on the possibility of tuning the self-assembly behavior of the system with temperature and composition of the solvent mixture.

1. Introduction

Block copolymers (BCPs) are polymers composed two or more blocks, which are often immiscible but covalently bound together. BCPs have attracted considerable attention for many decades due to their unique surface activity and the ability to self-assemble. The ability of BCPs to self-assemble into different morphologies renders them suitable candidates for biomedical applications[1], especially for drug delivery system[2]. Hydrophobic drugs can be encapsulated in the core of the assemblies and transported at concentrations that exceed their intrinsic solubility[3]. Meanwhile, the hydrophilic corona can be functionalized by functional groups to target specific position in vivo and release the drugs afterwards. Another area of potential applications of BCPs is based on the surface activity, which is the ability to lower the surface tension at the interfaces. With the strong tendency of distributing at the interface of two immiscible phases, the amphiphilic block copolymers can be used to modify interfacial properties, such as the wetting and biocompatibility, and even the to stabilize colloidal particles, such as the pigment particles in coating science[4].

Driven by the increasingly interests of BCPs, significant works have been focused on the synthesis of BCPs. Two types of polymerization have been developed, one is called step-growth polymerization that small molecules react with each other to form larger units so that the reactions can take place between monomers, oligomers and polymers[5]. However, this normally results in a broad molecular weight distribution due to the existence of oligomers throughout the reaction. Another one is called chain-growth polymerization, among which the ring opening polymerization (ROP) is one of its forms[6]. In the ROP reaction, the terminal end group of polymer chain acts as a reactive center so that a cyclic monomer can react with it via ring opening. To achieve the polymerization, one of the rings has to be opened first, which can be achieved in several ways. For instance, anionic ring-opening polymerization (AROP) is initiated by a small amount of nucleophile (Lewis base), while electrophilic reagents (Lewis acid) can initiate the polymerization by so-called cationic ring-opening polymerization (CROP). The ROP mechanism can also proceed via free radical polymerization (RROP)[7]. Controlled ROP enables us to synthesize well-defined polymers with controlled chain length and polymer architectures, such as block copolymers[8], graft copolymers[9] and star-shaped polymers[10].

1.1 Properties of block copolymers

1.1.1 Self-assembly

Self-assembly of BCPs in bulk with immiscible blocks have been studied in both experimental and theoretical aspects since the 1960s[11]. In the self-assembly process, the BCPs experience a micro-

phase separation due to the immiscibility of the constituent blocks. However, the covalent bonds between the blocks prevent them from separating macroscopically, resulting in a self-assembly of BCPs into variety of morphologies, such as spheres, cylinders, bicontinuous gyroids and lamellae[12]. These morphologies are mainly determined by three important parameters: the total number of repeating units (N),i.e. the degree of polymerization, the relative volume fraction of the blocks (f) and the Flory-Huggins interaction parameter (χ), which describes the enthalpic deviation from ideal mixing[13].

Compared with the situation in bulk, the self-assembly of BCPs in solution is more complex, as the interaction between solvent and constituent blocks plays a fundamental role. When the amphiphilic block copolymers are in a selective solvent, the lyophobic blocks tend to rearrange themselves in order to minimize the contact with the solvent. Driven by this minimization of interfacial energy, the self-assembly starts to occur. As the BCPs start aggregating, the interfacial area between the lyophobic block and the solvent decreases resulting in a decrease of the interfacial free energy. However, with increasing number of chains aggregating, they start to feel each other's steric repulsion. To reduce the steric repulsion, the lyophilic chains try to expand and stretch towards the solvent. Nevertheless, the stretching of the chains over their equilibrium conformation results in a decreasing of the configurational entropy which is unfavorable, leading to an end of the self-assembly process.

The morphology of self-assembled structure is determined mainly by the balance among three contributions: the core-chain stretching, corona-chain stretching (entropic contribution) and the interfacial energy between the core and the solvent (enthalpic contribution)[13]. The steric repulsion between lyophilic and lyophobic chains is affected by the curvature of the interface between core and corona of the micelle (Fig.1). A higher curvature leads to more available space for the lyophilic chains, therefore the steric repulsion and the stretching of the lyophilic chains is relatively small in spherical morphologies (Fig.1(a)) and large for flat morphologies(Fig.1(b)). The curvature of the interface also affect the stretching of the lyophobic chains in the core. If the curvature of the interface is high, less space is available for the lyophobic chains resulting in a higher stretching in the spherical geometry than in the flat one.

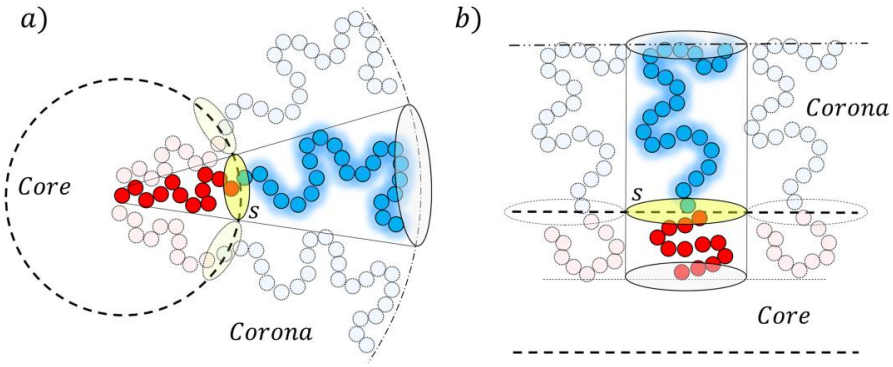

Fig.1. Schematic representation of a block copolymer in a spherical micelle (a) and a flat bilayer (b). The interfacial area between two blocks is noted in yellow[14].

The mostly studied aspect for controlling the morphology are the polymer-related properties, such as the relative length of blocks, copolymer composition and copolymer concentration. Among these, the relative length of hydrophobic and hydrophilic block is considered the most important parameter to gain control over the morphology of the aggregates[15]. Since the packing of assembled amphiphilic molecules is influenced by the geometry, the dimensionless packing parameter, p, has been defined by Israelachvili in 1976 to target specific self-assembled structures[16]. The packing parameter is defined as: $p = v/a_0 l_c$, where v, l_c is the volume and the length of the hydrophobic block respectively, a_0 is the surface area per copolymer molecule at the interface between hydrophilic and lyophobic block (Fig.2). As a general rule, spherical micelles are formed when $p < 1/3$; cylindrical micelles are formed when $1/3 < p < 1/2$; when $1/2 < p < 1$, flexible lamellae or vesicles are formed; $p = 1$ refers to planar lamellae and if $p > 1$, inverted structures can be obtained[17].

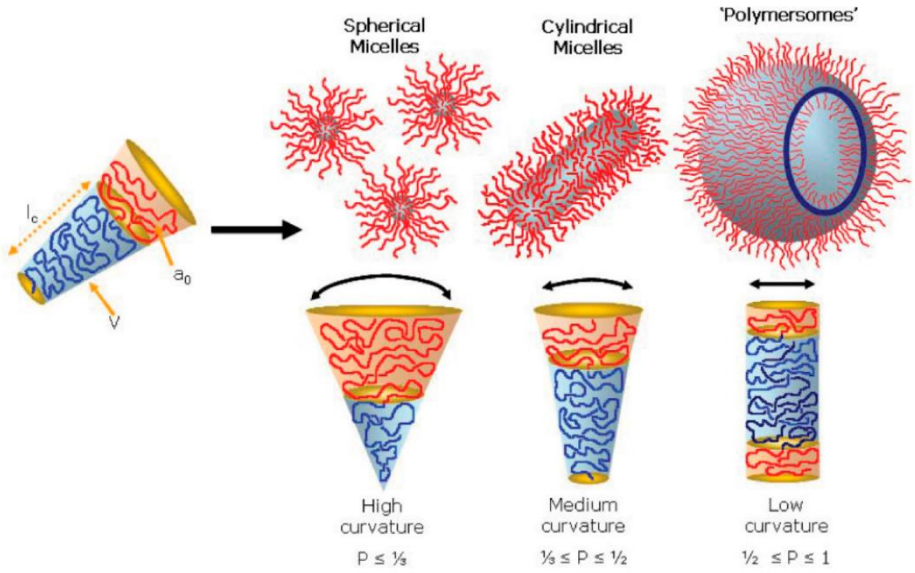

Fig.2. Various self-assembled structures formed by amphiphilic block copolymers in a block-selective solvent. The type of structure formed is due to the inherent curvature of the molecule, which can be estimated through calculation of its dimensionless packing parameter, p[18].

Apart from the polymer-related properties, the manipulation of solution conditions can also affect the morphology by changing the balance between the mentioned three contributions. It has been shown that the nature and composition of the solvent can affect the aggregate architecture. A. Eisenberg et al. have observed a series of morphological transition of polystyrene-b-poly (acrylic acid) block copolymer from spheres to rods, vesicles and bigger vesicles by increasing water content in the dioxane-water mixtures[19]. In addition, the morphological transitions via increasing

and decreasing water content are completely reversible. By changing the solvent properties the interfacial tension between the insoluble core of the assemblies and the solvent changes, this cause a rearrangement of the structure and a change in the balance between steric repulsion and stretching, causing a morphological transition that reduces the total free energy of the system[20].

Temperature has been also used as a tool to control the block copolymer self-assembly[21]. This temperature-dependent micellization and demicellization is specifically useful for temperature-driven drug delivery. Prachur Bhargava et al. have observed a reversible morphological changes of PS-b-PEO in DMF/water systems by changing the temperature[22]. Increasing the temperature from room temperature, the morphology changed from vesicles to worm-like cylinders and then to spheres with mixed morphologies in between. Moreover, no hysteresis was found in the morphological changes achieved by heating and cooling the system. Aydin Can and coworkers have shown that it is possible to gain control over the self-assembly of polystyrene-block-poly(methyl acrylate) (PS-b-PMA) in water-ethanol mixtures, obtaining switchable micellar structures upon changing the temperature[23] [24]. This shows that it is possible to induce thermoreponsive properties by changing the solvent composition.

1.1.2 Phase behavior

The phase behavior of a polymeric system can be described with the Flory-Huggins mean-field theory, a well-known model that describe the thermodynamics of polymer solutions and polymer blends[25]. The solvent and polymer repeating units are considered to have the same size. In a polymer-solvent system, N_p polymers, composed of N repeat units and N_s solvent molecules are distributed over a lattice, with the segment volume fraction of $\varphi_\mathrm{p} = N_\mathrm{p}\mathrm{N}/N_\mathrm{tot}$ and $\varphi_\mathrm{s} = 1 - \varphi_\mathrm{p} = N_\mathrm{s}/N_\mathrm{tot}$ respectively (N_tot is the total number of sites composing the lattices). The following expression for the entropy of mixing, ΔS_mix is used:

$$\Delta S_\mathrm{mix} = -k_\mathrm{B}[N_\mathrm{p} ln\varphi_\mathrm{p} + N_\mathrm{s}\ln(1-\varphi_\mathrm{p})] \quad (1)$$

Flory and Huggins introduced a new parameter, called χ-parameter, to describe the polymer-solvent interaction: $\chi = \frac{\Delta H_\mathrm{mix}}{k_\mathrm{B}\,T\,N_\mathrm{s}\varphi_\mathrm{p}}$, which is related to the heat of mixing (enthalpy part), $\Delta G_\mathrm{mix} = \Delta H_\mathrm{mix} - T\Delta S_\mathrm{mix}$. By combing the entropy part with the enthalpy part, the Gibbs free energy of mixing, ΔG_mix, can be obtained:

$$\frac{\Delta G_\mathrm{mix}}{k_\mathrm{B}\,T} = N_\mathrm{p} ln\varphi_\mathrm{p} + N_\mathrm{s}\ln(1-\varphi_\mathrm{p}) + \chi N_\mathrm{s}\varphi_\mathrm{p} \quad (2)$$

Then the free energy of mixing per lattice site can be written as:

$$\frac{\Delta G_\mathrm{mix}}{N_\mathrm{tot}k_\mathrm{B}\,T} = \Delta g_\mathrm{mix} = \frac{\varphi_\mathrm{p}}{N} ln\varphi_\mathrm{p} + (1-\varphi_\mathrm{p})\ln(1-\varphi_\mathrm{p}) + \chi(1-\varphi_\mathrm{p})\varphi_\mathrm{p} \quad (3)$$

The dissolution of polymer is expected when the free energy shows a negative value($\Delta g_\mathrm{mix} < 0$). In most of the case, the χ-parameter is positive, so that ΔH_mix is also positive, so the value of

χ-parameter affects the free energy of mixing and determines whether the polymer solution experience a phase separation or remain homogeneous. If the value of χ-parameter is high, phase separation will occur, as the entropic contribution is not sufficient to compensate the unfavorable enthalpy change. In contrast, only one phase is presented if the value of χ-parameter is low.

In the plot of the free energy of mixing ΔG_{mix} as a function of the segment volume fraction of one of the components φ (Fig. 3), the shape of $\Delta G_{\mathrm{mix}}(\varphi)$ curve varies as the value of χ (related to the temperature) changes. This plot provides a graphic prediction of when the polymer solution experiences a phase separation. At high value of χ (lower temperature) the phase separation is favorable due to the appearing of these two minima. Any mixture with a composition between these two concentrations will spontaneously phase separate into phases of composition φ_A and φ_B, which are the points of the common tangent as illustrated in dash lines (Fig. 3). The binodal curve is defined by the points of common tangent to ΔG_{mix} as a function of temperature. The slope of the tangent to the free energy curve provides the chemical potential $\mu_i{}^* = \mu_i/(kT)$ from the relation

$$\mu_i = \frac{\partial G_{\mathrm{mix}}}{\partial N_i} \tag{4}$$

At the composition φ_A and φ_B, the chemical potential are equal and two phases can coexist. As a result, for the coexistence phases A and B we can get $\mu_{\mathrm{p}}{}^A = \mu_{\mathrm{p}}{}^B$ and $\mu_{\mathrm{s}}{}^A = \mu_{\mathrm{s}}{}^B$. To construct a phase diagram, χ-parameter has to be calculated in terms of chemical potentials, then by plotting the temperature (related with χ -parameter) with the composition φ_{p} for a homogeneous mixture of polymers and solvent, a phase diagram can be obtained, shown in Fig.4. The point that satisfied the following condition is called the critical point:

$$\frac{\partial^2 g_{\mathrm{mix}}}{\partial \varphi^2} = 0 \qquad and \qquad \frac{\partial^3 g_{\mathrm{mix}}}{\partial \varphi^3} = 0 \tag{5}$$

From their solutions a critical χ-parameter can be obtained:

$$\chi_c = \frac{1}{2}\left(1 + \frac{1}{\sqrt{N}}\right)^2 \tag{6}$$

This illustrates that the molecular weight of polymer also plays a role in the critical interaction parameter. An increase in polymer length (larger N) will decrease the value of critical χ-parameter and consequently the phase separation will become more favorable. Meanwhile, the χ-parameter is generally a function of inverse of temperature, which means the solubility increases with temperature. This provides a possibility to cross the critical point by tuning the temperature, giving rise to the upper critical solution temperature (UCST) behavior (Fig.4, a).

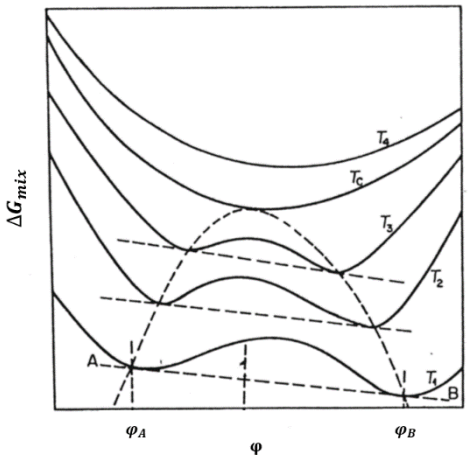

Fig.3. Gibbs free energy as a function of composition at different temperatures, and the corresponding phase diagram showing the binodal curve (dash curve).

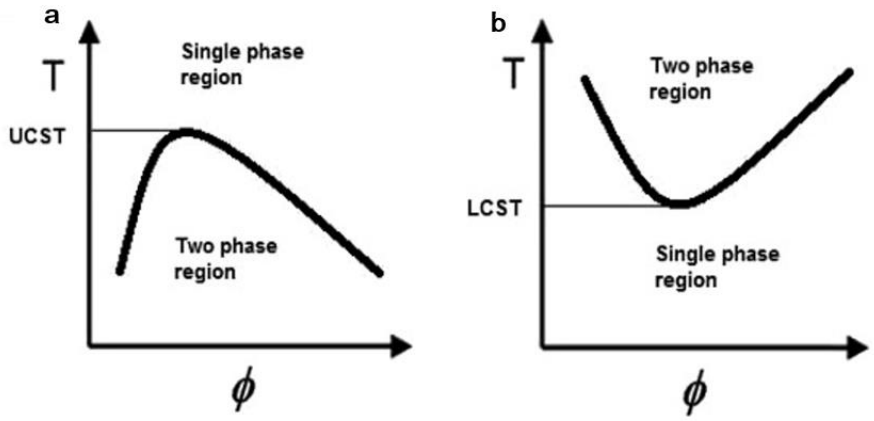

Fig.4. Typical phase diagrams for a polymer solution with a lower and upper critical solution temperature[26].

The upper critical solution temperature (UCST) is the critical temperature above which the components of a mixture are miscible in all proportions. Below the mixing region, polymer chains undergo a transition from open coil to the globule state. If the globule state is not stable, subsequently, the aggregation occurs and form visible particles which cause turbidity. As a results the sedimentation will cause phase separation into a polymer-rich and a polymer-poor phase.

The lower critical solution temperature (LCST) behavior (Fig.4, b) occurs when the χ parameter increase with increasing temperature. A polymer exhibiting a LCST behavior in solution mainly because of the loss of hydrogen bonded solvent molecules. High temperatures weaken the hydrogen bonds, leading to the release of solvent molecules (entropy driven desolvation), which results in phase separation.

The points of a phase diagram different from UCST and LCST are generally called the cloud point temperature T_{cp}, the temperature at which the phase transition of a polymer solution at a specific concentration occurs[27]. The value of T_{cp} changes with concentration, solvent composition and ionic strength[28].

1.1.3 Crystallization

Polymer crystallization is a process by which the polymer chains undergo a transition from random coil to fully extend or folded conformation. This results in the formation of a basic crystalline lamellar structure, which further grow radially to form a spherulitic crystalline structures at a larger scale. Normally, polymers do not fully crystallize and only form partial crystalline structures, i.e. semi-crystalline structures, because of the dispersity in molecular weight and imperfect alignment of chains. If a polymer does not exhibit any crystalline structure, then it is defined as amorphous polymer. The crystallization of polymer can be induced in various ways, upon cooling from the melt, mechanical stretching[29] and solvent evaporation[30].

The crystallization process become more interesting with the presence of multiple blocks. Crystallization in homopolymers leads to an extended conformation, or to kinetically controlled chain folding. In block copolymers, on the other hand, equilibrium chain folding can occur, the equilibrium number of folds can be controlled by the molecular weight of the second noncrystallizable block[31]. The combination of amorphous-amorphous, amorphous-crystalline, crystalline-crystalline components in BCPs lead to a wide variety of mechanical and structural properties, comparing with homopolymers[32]. Among those combinations, the one containing both crystallizable blocks become increasingly important in polymer science, because the interplay between crystallization and mirco-phase separation can strongly affect the crystalline structures, morphologies in larger scale and properties of the materials[31]. The immiscibility of blocks force them to separate from each other, however, the covalently bound blocks hinder the separation at the same time, which finally induces a mirco-phase separation. The size and morphology of the mirco-domines can be tuned by the molecular weight and the crystallizability of each block[33].

1.2 PEO-b-PCL block copolymers

1.2.1 Properties and applications

Recently, there has been considerable interest in developing biodegradable and biocompatible amphiphilic block copolymer for in vivo drug delivery, due to their ability of self-assembly into various morphologies, which can host and deliver hydrophobic compounds. Among the BCPs,

Poly(ethylene oxide)-block-poly(ϵ-caprolactone) diblock copolymers (PEO-b-PCL) has been regarded as an ideal BCP for this application, by considering the unique properties of each single block. Apart from the low toxicity of PEO, it also has a unique 'stealth' property, which is the ability to avoid to be recognized by the immune system. Moreover, the PEO corona resists protein adsorption and cellular adhesion, protecting the hydrophobic drug against hydrolysis and enzymatic degradation. PEO also shows a high solubility in both water and in organic solvent, and its end groups can be functionalized for targeting[34]. The combination of biodegradability and biocompatibility of the hydrophobic block PCL also makes it a great candidate for biomedical applications, and its high hydrophobicity make it a good host for insoluble drugs.

1.2.2 Behavior in water and alcohol of the single blocks

In a great extent, the behavior of the PEO-b-PCL block copolymer depends on the behavior of the single building blocks, PEO and PCL. The phase behavior of PEO in water and in alcohol will be discussed respectively as well as the crystallization behavior of PEO and PCL.

PEO has been widely used as a hydrophilic biomaterial, and the aqueous PEO solutions also exhibit an unusual behavior which is the formation of a so-called closed-loop phase miscibility[35]. This means PEO in water has both UCST at high temperatures and LCST at low temperatures. Suk Yung Oh and coworkers have shown the closed-loop phase diagram of PEO in water by comparing the calculated results and experimental results, and the calculation curves fit fairly well to experimental data which shown in Fig.5[36].

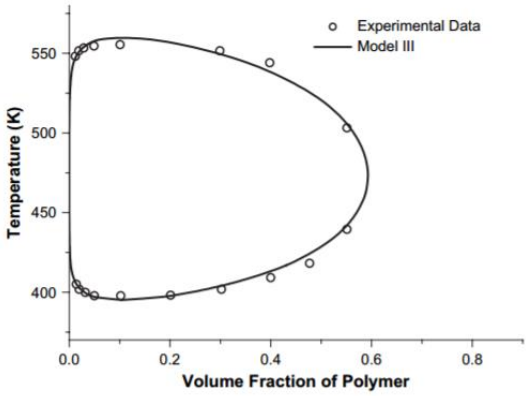

Fig.5. Coexistence curves for PEO/water system, the open circles are experimental data for PEO molecular weight of 8000, the solid lines are calculated results.

It also has been reported that PEO also exhibit an unusual behavior in alcohol. Recently, Derek L. HO and coworkers found out that in ethyl alcohol PEO exhibits regular polymer solution thermodynamic behavior with an upper critical solution temperature phase diagram. However, the boundary of the UCST phase is significantly below the melting temperature, which indicates the system undergoes a crystallization process before the phase separation can occur upon cooling,

resulting in an unusual phase transition[37].

Bearing such competition between phase separation and crystallization, it is reasonable to investigate the crystallization behavior of the polymer in solution. Both PEO and PCL are crystallizable polymers, however, the structure of the crystals at different crystallization condition shows a great variety. Crystallization from dilute solution leads to well defined crystal structures, which is because the polymer chains are isolated and unentangled in dilute solution. As a result, the probability to be incorporated together is much less compared to polymer crystallization from the melt. The single crystal of PEO with a square shape lamellar crystal and PCL with a hexagonal shape have been observed via crystallization from their dilute solution in hexanol[38]. Melt-grown PCL crystals showed a truncated lozenge lateral shape, with curved or chair-like three-dimensional morphology. Similar lamellar morphologies were observed in larger crystal aggregates, i.e. hedrites, grown at lower crystallization temperatures in the melt. The individual lamellae in these crystal aggregates also showed an elongated truncated lozenge shape[39]. PCL main reflections are located in 2θ at 21.40°, 22.05° and 23.7° corresponding to the (110), (111) and (200) reflections, PEO crystallizes in these compounds in the triclinic system and he most intense peaks appear at 19.2° and 23.5° [40].

1.2.3 Behavior in water and alcohol of PEO-b-PCL copolymer

The properties of PEO-b-PCL copolymer are different from the properties of the single blocks. As a result, it is crucial to understand how the PEO-b-PCL copolymer arrange themselves in different solution conditions, as well as their phase and crystallization behaviors.

PEO-b-PCL exhibits a UCST behavior in ethanol, which is exploited as a purification method for the PEO-b-PCL synthesis[41]. However, the behavior of PEO-b-PCL in water-ethanol mixtures are less explored.

After understanding the crystallization behavior of single blocks, it is of great importance to study the crystallization process of PEO-b-PCL in solution as well as in bulk. What makes the PEO-b-PCL system interesting is that the glass transition temperature T_g (around -60℃), the crystallization temperature T_c and the melting temperature T_m (around 60℃) of the two components are very similar. This is not the case in most of the crystalline-crystalline diblock copolymer systems, where the melting temperature difference between the two blocks is quite large[42]. The crystallization of PEO-b-PCL diblock copolymer is of course different from that of individual blocks, because of the chain connectivity of the block copolymer. The crystallization of one block may hindered by the other, which leads to the imperfect crystallization. This can be confirmed by the decrease in crystallinity and the depression of copolymer melting temperature as compared to the individual

blocks[43].

Moreover, the morphology of crystalline structure can be influenced by many factors. For instance, the relative block length, crystallization temperature, presence of solvent and solvent composition, when crystallization in solution occurs. The crystallization behavior and morphology of PEO-b-PCL diblock copolymers with different block length were studied by Chaoliang He and coworkers[44]. The block with larger molecular weight crystallizes first and leads to imperfect crystallization of another block. Moreover, the spherulitic structures of PEO-b-PCL copolymers with different block length ratio were also observed by polarized optical microscopy. Besides, H.S.Kim has classified the PCL-PEO-PCL triblock copolymer into three groups via relative block length: PCL dominant crystallization, PEO dominant crystallization and competing case when the length of the blocks are almost equal. Among these, the latter case is more complex, involving the strong dependency on thermal history crystallization[45]. Apart from the block length, crystallization temperature is also a significant factor that affect the crystallization properties of PEO-b-PCL block copolymer.

During solution crystallization, lamellar crystals are formed from dilute solution, usually via self-seeding technique, with the second block tethered on the basal surface. Once the crystallization occurs upon cooling the solution, one block will crystallize preferentially, depending on the solvent quality or molecular weight. Then the local concentration of the first block will increase, and the conformation of the second block will be driven by this solvent interactions. It has been confirmed that the morphology of PEO-b-PCL in hexanol exhibits an elongated hexagonal shape which is similar to the hexagonal shape of PCL crystal rather than a square-shaped PEO crystal[38]. This is due to the preferential crystallization of PCL in hexanol lamellar single crystal are formed, followed by the crystallization of PEO block on the surface of PCL lamellar crystal, eventually results in a three-layer structure.

1.3 Properties of water-ethanol solvent mixtures

Water-ethanol solvent mixtures are environmentally friendly low-toxicity solvents that exhibit abnormal properties due to the presence of hydration shells around the ethanol molecules. The presence of such hydration shells has been reported to result in solubility maximum for drug molecules in water-ethanol mixtures[46]. This is due to the interaction between water molecules and ethanol, which makes the mixtures different from the individual solvents for drug molecules. In the model of Frank and Wen[47], the water molecules in pure liquid water are ordered in self-stabilizing, three dimensional, hydrogen-bonded clusters. The addition of an alcohol into water can disrupt the network of hydrogen-bonded water molecules, resulting in the formation of structures where ethanol molecules are surrounded by cages of water molecules. However, increasing the amount of alcohol into water, the network of water clusters is broken into disconnected water

clusters. Further adding alcohol leads to the disruption of the water clusters, results in the trimers, dimers and eventually free water molecules. Due to the unique structures of water-ethanol solvent mixtures, it is of great interests to study how the polymer behave in such system. For instance, the solubility of 2-methyl-2-oxazoline-block-2-phenyl-2-oxazoline (MeOx-PhOx) diblock copolymer in water-ethanol mixtures was studied by tuning the composition of the solvent mixtures, which leads to increased solubility, a critical micelle solvent composition, stable dispersions and LCST transitions followed by an UCST[48]. Moreover, polymers with UCST behavior in the water-alcohol solvent mixtures are reported as potential biomedical and 'smart' materials[46].

2. Experimental methods

2.1 Materials

The precursors Poly(ethylene glycol) methyl ether (PEO2000, Mw=2000), Polycaprolactone diol (PCL2000, Mn=2000), ε-caprolactone monomer and Acetyl tributyl citrate (ATBC) were obtained from Sigma Aldrich. Fumaric Acid was purchased from Fluka and absolute ethanol and acetone were from Biosolve, the Netherlands. All the glassware was dried in the oven at 100℃ for 24h.

2.2 Synthesis, purification and characterization of PEO-b-PCL

2.2.1 Synthesis

A one-pot, solvent free and metal free synthetic method has been used to prepare the PEO-b-PCL block copolymer[41]. A high degree of conversion and narrow polydispersity have been obtained via the ring opening polymerization of ε-caprolactone, in which the furmaric acid acts as catalyst and mono-poly(ethylene oxide) as initiator. The synthesis of copolymer involves three steps: dehydration of the precursors, polymerization reaction and purification.

The synthetic steps of PEO2000-PCL1400 are the following: first, 2g PEO2000 (1mmol) and 0.69g furmaric acid (6mmol) are heated at 125℃ under Nitrogen flow in a 50ml two-neck flask, in which a magnetically coupled collapsible blade stirrer is installed. Then the dry nitrogen was pumped into the mixture by a long dry needle for 1h through the secondary neck, which was sealed with a rubber stopper. The resulting mixture was then cooled down to 90℃ and 1.4g ε-caprolactone (12 mmol) was added quickly while stirring. The mixture was stored in closed flask at 90℃ for 24h under Nitrogen flow.

2.2.2 Purification

PEO-b-PCL block copolymer exhibits a UCST behavior in ethanol, which allows us to use a purification process based on this property. As mentioned in section 1.1.2, a system with UCST behavior will undergoes a miscible to immiscible transition when lowing the temperature below UCST. Phase separation will occur and allowing us to separate the polymer-rich phase from the polymer-poor phase.

When the desired degree of polymerization was reached, 40ml ethanol was added and the mixture was heated up to 60℃ under stirring until dissolution. The mixture was then cooled to room

temperature and stored at -18℃ in a freezer until the polymer precipitation occurred. The precipitate was then filtered in Buchner filtration system, washed with cold (-18℃) ethanol and finally dried in vacuum.

2.2.3 Characterization

The characterization of synthesized copolymer was performed by Nuclear Magnetic Resonance (NMR) and Gel Permeation chromatography (GPC). ^{1}H NMR analysis was carried out on a Varian 400 (400 MHz) spectrometer at 25℃. The obtained spectra were used to verify the chemical structure and the degree of polymerization of the synthesized copolymers. The characterization used deuterated chloroform with TMS reference as solvent. In Fig.6, the presence of the triplet at 4.22 ppm (d) is associated to the protons relaxation in the terminal –O-CH_2– units in PEO block which indicates the successful functionalization. The ratio between the integrals of the signal associated to the protons relaxation in the terminal –O-CH_3 units in PEO block (a, 3.37 ppm) and the one associated to the relaxation of –O-CH_2– proton in the open Ɛ-caprolactone (i, 4.06 ppm) were used to calculate the synthesized copolymer's degree of polymerization, thus the average mass ${M_n}^{NMR}$. The calculate molecular weight (3370 Da) of the copolymer is in a good agreement with the value we expected (3400 Da).

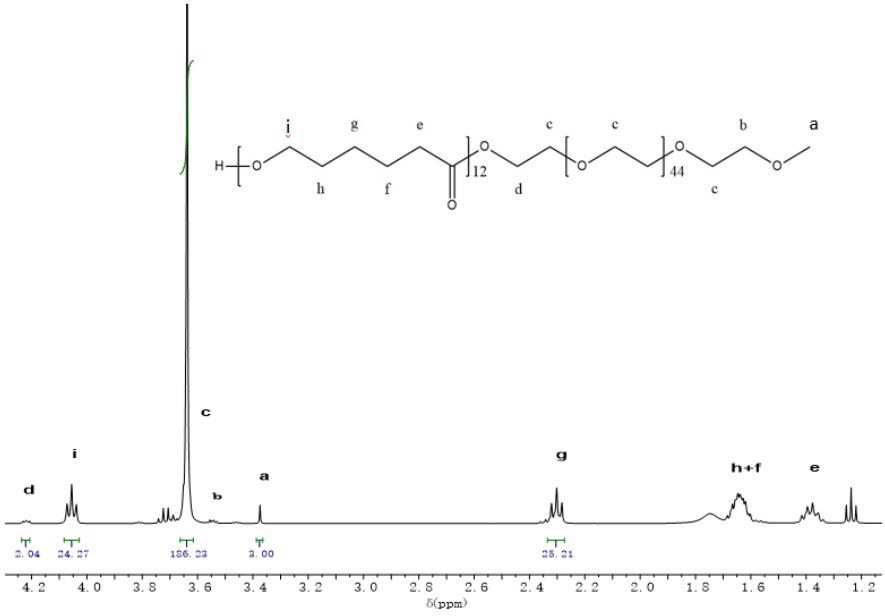

Fig.6. ^{1}H NMR spectra of PEO2000-PCL1400.

Gel Permeation Chromatography (GPC) was used to evaluate the molar mass dispersity ($Đ = {M_w}^{GPC}/{M_n}^{GPC}$) of the copolymers. THF was selected as eluent and a set of two mixed bed columns (Mixed-C, Polymer Laboratories, 30 cm, 40 C) was used. The system was calibrated using narrow molar mass polystyrene standards ranging from 600 to 7106 Da. The GPC result (Fig.7) shows a narrow polydispersity of 1.07 for the synthesized PEO2000-PCL1400 block copolymer.

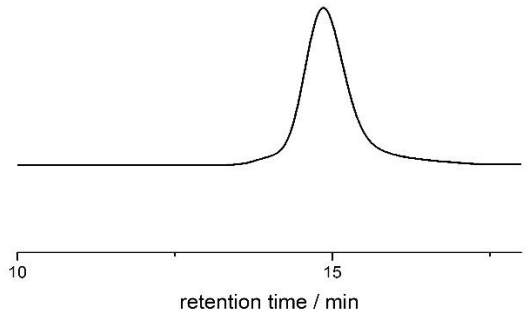

Fig.7. The GPC profile of PEO2000-PCL1400 block copolymer.

2.3 Analysis of PEO-b-PCL in ethanol and water-ethanol mixtures

2.3.1 Turbidimetry

In section 1.1.2, the phase diagram of polymer with UCST and LCST was discussed. As mentioned, the cloud point, T_{cp} , is defined as the temperature when polymer phase separation occurs at a specific concentration.

Turbidimetry is an extensively used method to measure the cloud point of a polymer solution. The basic principle is to measure the intensity of transmitted light through a cuvette that containing a polymer solution. When the phase separation occurs, the transmittance of the sample will shows a dramatic decrease due to the scattering effect of the demixed polymer phase.

Turbidity measurement were performed with a HP 8453 UV-vis spectrophotometer, equipped with a Peltier plate to ensure the accuracy of temperature control. For this study, the measurements were carried out at a wavelength of 700nm upon heating (steps of 2℃ from 0 to 60℃)and cooling (steps of 2℃ from 60 to 0℃) . Several samples of PEO-b-PCL in water-ethanol mixtures (5%wt) with different water content (50 vol%, 40 vol%, 30 vol%, 20 vol%, 10 vol%, 5 vol%, 1 vol% and 0 vol%, where 0 vol% represents for the pure ethanol solvent) were prepared for this measurement. The polymer solutions were first stored in the freezer at -18℃for 20min before the measurement. For the measurement upon cooling, samples were first placed in the thermostats at desired temperature for 20 min in order to reach the equilibrium. Then the absorbance of the light is measured as a function of temperature by UV-vis spectrophotometer (Fig.8, top). The cloud points are obtained by taking the maxima of the derivative (Fig.8, bottom), the polymer solution of 0 vol%

water (pure ethanol) upon cooling and heating are shown as examples.

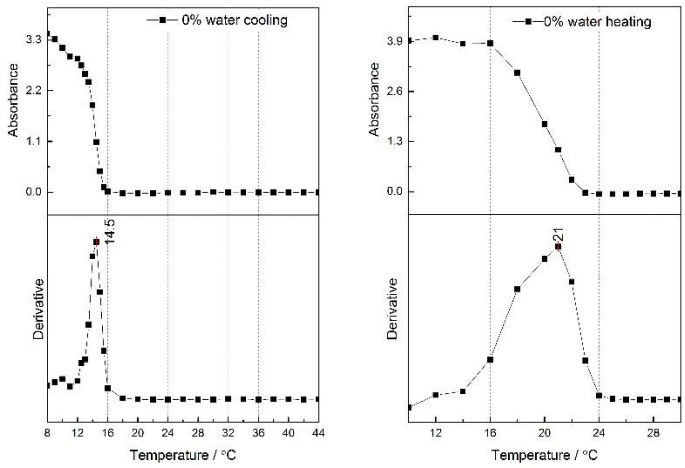

Fig.8. Absorbance as a function of temperature for PEO2000-PCL1400 in pure ethanol upon cooling and heating (top), the derivative of the upper function for the determination of cloud points (bottom).

2.3.2 Differential Scanning Calorimetry (DSC)

Differential Scanning Calorimetry (DSC) is traditionally used to study the thermophysical properties of polymers, by measuring the difference in heat flow rate between a sample and inert reference as a function of time and temperature. For example, during the melting, since it is an endothermic process, extra heat is required to maintain the sample at the same temperature as set in the DSC. However, crystallization process is an exothermic process, which means less energy is required. The DSC can be used to measure the glass transition temperature, melting point and crystallization temperature of polymers.

DSC measurements were carried out by a TA instrument Q1000 differential scanning calorimeter. Samples consisting of 5%wt (50mg/ml) dispersion of PEO2000-PCL1400 block copolymer in the different solvent mixtures were measured at temperature range from -50℃ to 65℃, with scanning rate of 1℃/min and the samples were equilibrate at maximum and minimum temperature for 5min. Different solvent mixtures and PEO and PCL homopolymers have been measured under same condition as reference. The thermal behavior of polymer solution with additive is also studied by DSC, where 1ul (6 ATBC molecules per PEO-b-PCL polymer chain) additive ATBC is added in different polymer solution during sample preparation. Before measuring, all the samples were placed in the oven at 65℃ for 2h to ensure that the pans and the lids were well sealed.

2.3.3 Static Light Scattering and Dynamic Light Scattering (SLS and DLS)

Scattering techniques are powerful tools in the characterization of molecular structures in colloidal system. Several quantitative information can be obtained, such as size, shape, structure and interactions of polymer coils, micelles or larger particles. In general, the technique is based on the interactions between the incident radiation and the particles in solution. The length scale of the measurement that are probed is determined by a so-called wave vector, q which is related to the scattering angle θ via:

$$q = \frac{4\pi n_D \sin(\frac{\theta}{2})}{\lambda} \qquad [m^{-1}] \tag{7}$$

Where λ is the wavelength of the laser light and n_D is the refractive index of the solvent itself. Thus, by varying either θ or λ, different length scale can be probed.

In diffraction experiments, will be discussed in section 2.3.4, the scattering angle is set to 2θ, so that the distance probed d is proportional to q via:

$$d = \frac{2\pi}{q} \tag{8}$$

Dynamic light scattering (DLS) is a light scattering technique that characterizes the diffusion of particles in solution. The movement of particles will cause fluctuations in the scattered intensity with time, which is directly related to the Brownian motion of the scattering particles. This mobility is related to the diffusion coefficient, D and is further related to the hydrodynamic radius R_h of the particles through the Stokes-Einstein equation:

$$D = \frac{k\,T}{6\pi\eta R_h} \tag{9}$$

Where k is the Boltzmann constant, η is the viscosity of the solvent.

To understand DLS in detail, the intensity autocorrelation function $g_2(\tau)$ will be illustrated, which express the scattered intensity fluctuations in terms of delay time τ dependence of intensity autocorrelation functions:

$$g_2(\tau) = \frac{<I(t)\times I(t+\tau)>}{<I(t)>^2} \tag{10}$$

This intensity autocorrelation function gives information about to which extent the scattering intensities are coupled as a function of delay time. If τ is small, $I(t+\tau)$ and $I(t)$ are still strongly coupled, since they are almost the same. However, with a large delay time, the correlation between the two is decreased or even lost. The intensity fluctuations arise from phase fluctuations of the electromagnetic waves, which tells the change in positions of particles with time. Since the intensity of the light scales with the square of the amplitudes of the electromagnetic wave, it is

reasonable to relate $g_2(\tau)$ to the electric field autocorrelation function, $g_1(\tau)$, through Siegert relation[49]:

$$g_2(\tau) = 1 + \beta[g_1(\tau)]^2 \tag{11}$$

where β is an experimental constant which depends on the geometry of the setup and the coherence of the laser and the value is equal to or lower than unity. $g_1(\tau)$ is related to the decay rate of the autocorrelation function Γ, which tells how fast the correlation disappears. For monodisperse spherical particles, $g_1(\tau)$ decays exponentially as follows:

$$g_1(\tau) = e^{-q^2 D\tau} \tag{12}$$

When we combine eq.(11) and eq.(12) and plot $ln\sqrt{(g_2(\tau) - 1)}$ versus τ, a linear relation is obtained, and the decay rate Γ can be obtained from the value of the slope. Since the decay rate is related to D by $\Gamma = q^2 D$, the diffusion coefficient can be calculated from Γ. To be notice, this relation is only suitable for dilute dispersion, where there is no particle-particle interactions and only single scattering occurs.

Static light scattering (SLS) can be used to determine the molecular weight M_w, the radius of gyration R_g of polymer and the second virial coefficient A_2, which describes the interaction between scatterers. Several factors play a role in the intensity of scattered light, involving the scattering volumepvt, the detector distance, the particle volume and the wavelength of the scattered light. The absolute scattered intensity is also called Rayleigh Ratio R_θ that can be expressed as:

$$R_\theta = KCMP(q)S(q) \tag{13}$$

where $P(q)$ is called form factor, which is a corrected factor for the large particles since they can result in a multi-scattering within the same particle; the structure factor $S(q)$ account for the interparticle interference, aiming when the interaction between particles appears. K is an optical constant. M is the molecular weight of polymer in solution and C is the weight concentration. Experimentally, the Rayleigh Ratio is determined by the equation:

$$R_\theta = \frac{I(\theta)_{sample} - I(\theta)_{solvent}}{I(\theta)_{reference}} \times R_{reference} \times \frac{n^2{}_{solvent}}{n^2{}_{reference}} \qquad [m^{-1}] \tag{14}$$

Where $n_{solvent}$ and $n_{reference}$ are the refractive index of the solvent and the reference (usually toluene $n_{toluene} = 1.494$). $R_{reference}$ is the absolute scattering of the reference, which is used as correction value, and it is the function of λ: $R_{toluene} = \frac{4.9\times10^8}{\lambda^{4.17}}$.

For diluted particles (no interparticle interaction) with $qR \ll 1$, the so-called Guinier approximation can be used to measure the radius of gyration R_g:

$$ln(R_\theta) = 1 - \frac{q^2 {R_g}^2}{3} \tag{15}$$

The radius of gyration can be calculated from the slope of $ln(R_\theta)$ versus q^2 plot, which is known as Guinier plot. Note that the Guinier approximation should be strictly valid only for small values

of qR, where $qR < 1$.

The shape of the particles is another useful information that can be derived from the light scattering measurement. Two parameters that related to the topology of particles will be described, fractal dimension of particle d_f and the shape factor ρ-ratio.

In general, for any particles of a certain topology the mass scales with its size as: $M \propto R^{d_f}$. The scattered intensity of a particle is given as

$$logI(q) = -d_f \times logq \tag{16}$$

and it is valid for the regime of $qR > 1$. If $logI(q)$ is plotted vs $logq$, one obtains a linear decay with slope d_f, allowing to directly determine the fractal dimension of the scattering particle. Several fractal dimensions of some important particle topologies have been summarized[49].

Table1. Fractal dimensions of selected topologies

Topology	Fractal dimension $\boldsymbol{d_f}$
Cylinders, rods	1
Ideal Gaussian coil	2
Gaussian coil with excluded volume	5/3
Branched Gaussian chain	16/7
Swollen branched chain	2
2D-objects with smooth surfaces	2
2D-objects with fractal surfaces	1-2
3D-objects with smooth surfaces	3
3D-objects with fractal surfaces	2-3

The shape factor ρ-ratio provides important indication of the particle topology, typically for the particles with radius range from 10-100nm. The ρ-ratio can be quantity derived from gyration radius and hydrodynamic radius which determined from static and dynamic light scattering. It is simply defined as:

$$\rho = \frac{R_g}{R_h} \tag{17}$$

Theoretical values of the ρ-ratio of important particles topologies have been summarized to give a guide for determining the shape of particles[49].

Table2. ρ-ratio for the most-typical particle morphologies

Topology	**ρ**-ratio
Homogeneous sphere	0.775
Hollow sphere	1
Ellipsoid	0.775 - 4
Random polymer coil	1.505
Cylinder of length $\boldsymbol{l}$, diameter $\boldsymbol{D}$	$\frac{1}{\sqrt{3}}\ln(\frac{l}{D}-0.5)$

In our measurement, SLS and DLS were performed on ALV/CGS-3 Compact Gonimeter System with ALV/LSE-5004 Light Scattering Electronics and Mutiple Tau Digital Correlator. The wavelength of the incident light is 532nm. The scattering angles are measured ranging from 30° to 150°, with increment of every 10°.

2.3.4 Small Angle and Wide Angle X-ray Scattering (SAXS and WAXS)

Small Angle X-ray Scattering and Wide Angle X-ray Scattering (SAXS and WAXS) are the techniques where X-rays are scattered by the sample in the nm-range. The structural information that provided by SAXS is normally between 1 and 200nm, whereas WAXS can deliver information on a length scale lower than 1 nm, where typical Bragg diffraction peaks can be found. Compared to the conventional light scattering technique, the decrease in wavelength of incident light by X-ray source, allows to analyze the structure in a more detailed scale. Therefore, SAXS is normally use to probe supramolecular organization, WAXS is sensitive to atomic order (Bragg peaks).

Similar to the light scattering technique discussed above, the SAXS scattered intensity, $I(q)$ show different scaling regimes depending on the form factor of the object and the value of the scattering vector q (Fig.9). For $q << \frac{2\pi}{S}$, where S is the size of the scatteres, $I(q)$ is q independent (Guinier region). For value of $1/q$ comparable to S, $I(q)$ is proportional to the fractal dimension of the scatters. At higher q the scattered photons are mostly coming from the surface of the objects, and the scattered intensity scales with an exponent between 3 (rough surfaces) and 4 (flat surfaces). This scaling behavior is called Porod's law.

Therefore, in the Guinier regime the radius of gyration can be obtained form the slope of $\ln(I(q))$ versus q^2 plot. The fractal dimension can be calculated in the intermediate q region from a $\log(I(q))$ vs $log(q)$ plot. Finally, information about the surface roughness can be obtained in the Porod regime.

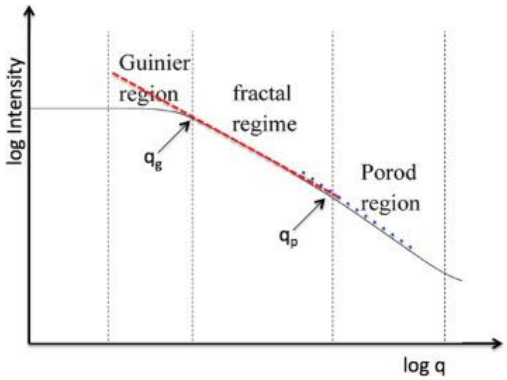

Fig.9. A generalized scattering curve[50].

Our SAXS and WAXS experiments were carried out with a Ganesha 300XL with $Cu\,K\alpha$ anode source (wavelength of 1.54056Å). Two configurations were measured for the q range of 0.008-0.29 Å and 0.088-2.41 Å for SAXS and WAXS respectively. The samples were measured at various temperature through step heating and cooling with rate of 2℃/min.

The scattered intensity is also influenced by the structure factor $S(q)$, which accounts for interferences related to the relative position of the scatterers. For the system with long range positional order, the structure factor is characterized by maxima, which are related with the dimension, repeating distances and symmetry of the structure. The relative position of the peak on the q-scale have typical values, which reveals the morphological symmetry of the diffracting lattice (Table3)[51].

Table3. The crystal symmetry and the corresponding ratio of peak position on wave vector.

symmetries	Ratio of peak positions
Lamellar	1: 2: 3…
Hexagonal	1: $\sqrt{3}$: 2: $\sqrt{7}$…
Body Center Cubic (BCC)	1: $\sqrt{2}$: $\sqrt{3}$: 2…
Face Center Cubic (FCC)	1: $\sqrt{3}$: 2: $\sqrt{8}$…

3. Results and discussion

3.1 Behavior in water-ethanol solvent mixtures of PEO and PCL homopolymers

The cooling and subsequent heating scan of PEO2000 and PCL2000 homopolymers in different solvent mixtures are shown in Fig.10 and Fig.11; the relevant temperatures and enthalpies are listed in Table4. In the case of PEO, both melting temperature and crystallization temperature (marked in red) decrease by increasing the water amount in the system. Moreover, the peak area related to the enthalpy change also decreases with the addition of water, which indicates the crystallization of PEO become more difficult by adding water. This is because the ethanol molecules (H-CH_2CH_2O-H) have the similar chemical structure with the PEO monomer [-(CH_2CH_2O)-] which induce the crystallization of PEO in ethanol. However, since water is a good solvent for PEO, the addition of water will increase the solubility of PEO in the solvent mixtures, therefore the mobility of the polymer chains become larger, so that PEO become more difficult to crystallize.

For PCL2000 homopolymer, the changing of both peak position and the peak area are not obvious by adding water, which means the effect of adding water on PCL crystallization is negligible. However, the shoulder of the crystallization and melting peaks which appears in pure ethanol start to immerge with the main peak by increasing the amount of water, but the total peak area remains almost the same. The reason can be that the water molecules form hydrogen bonds with the carbonyl groups in PCL which may affect only the arrangement of PCL chains when it crystallize, however the crystallinity does not change. The presence of two melting peaks of PCL is related to the different crystalline configurations[52].

Table4. DSC derived thermal data of homopolymers PEO2000 and PCL2000 in different solvent mixtures.

Samples	T_c(℃)	T_m(℃)	ΔH (J/g)	Samples	T_c(℃)	T_m(℃)	ΔH (J/g)
PEO (0vol%)	1.1	22	162.6	PCL (0vol%)	20.1	32.9	75.6
PEO (1vol%)	-1.2	21.5	151.5	PCL (20vol%)	22.4	34.8	74.5
PEO (5vol%)	-15.1	13.2	122.6	PCL (30vol%)	17.4	34.4	72.4
PEO (10vol%)		2.3	50.6	PCL (50vol%)	21.4	34.1	77.5

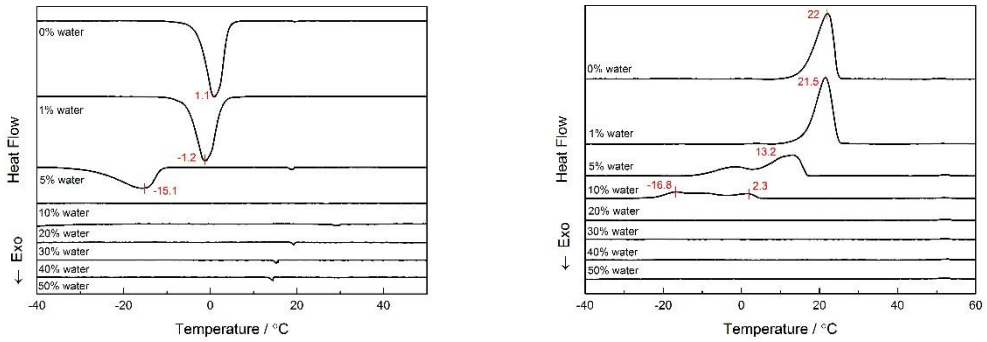

Fig.10. DSC cooling (left) and heating (right) scans of PEO2000 homopolymer in different solvent mixtures.

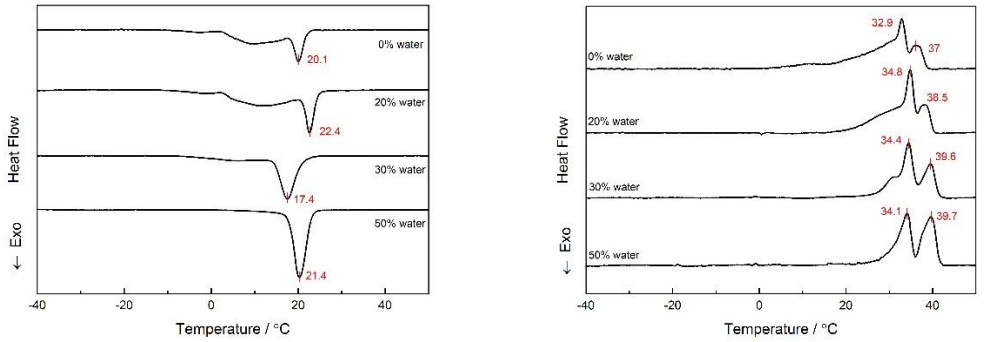

Fig.11. DSC cooling (left) and heating (right) scans of PCL2000 homopolymer in different solvent mixtures.

3.2 Behavior in water-ethanol solvent mixtures of PEO-b-PCL block copolymers

The cloud points were measured for PEO-b-PCL block copolymers in different water-ethanol solvent mixtures upon cooling (Fig.12) and heating (Fig.13). In order to gain a clear overview, the obtained cloud points were plotted as a function of vol% of water in the mixtures (Fig.14). Water is known as a worse solvent for PCL block compared with ethanol solvent, which means in theory the solubility of the PEO-b-PCL block copolymer should decrease with the addition of water, so that a directly increase of cloud points should be observed. However, a drop in T_{cp} can be observed until 10% water was added in the system, as shown in Fig.14. This interesting behavior is due to the non-ideality of the water-ethanol mixtures. When small amount of water was added in the ethanol, water-ethanol clusters are formed which changes the properties of the solvent. Moreover, compared with ethanol molecules, water molecules can form stronger hydrogen bonds with the block copolymer, which thus increase the solubility of the block copolymer in the mixtures. However, when the backbones of the PEO-b-PCL are fully occupied by the water molecules, the

additional water will not increase the solubility anymore. As a result, the cloud point increases after a certain amount of water is added.

To be noticed, there is a temperature difference between the obtained cloud points upon heating and cooling (Fig.14). A possible explanation could be that the dissolution process (upon heating) involves the formation of hydration layer around the copolymer chains which consumes energy. This energy depletion is mainly due to entropy loss when the block copolymers are surrounded by the water molecules. In comparison, the dehydration process is easier, so that less energy is required. Another possibility can be that the kinetic effect plays a role due to the larger cooling or heating rate compared to the dehydration or hydration rate. If the cooling or heating process is performed very slowly, the temperature difference could be reduced.

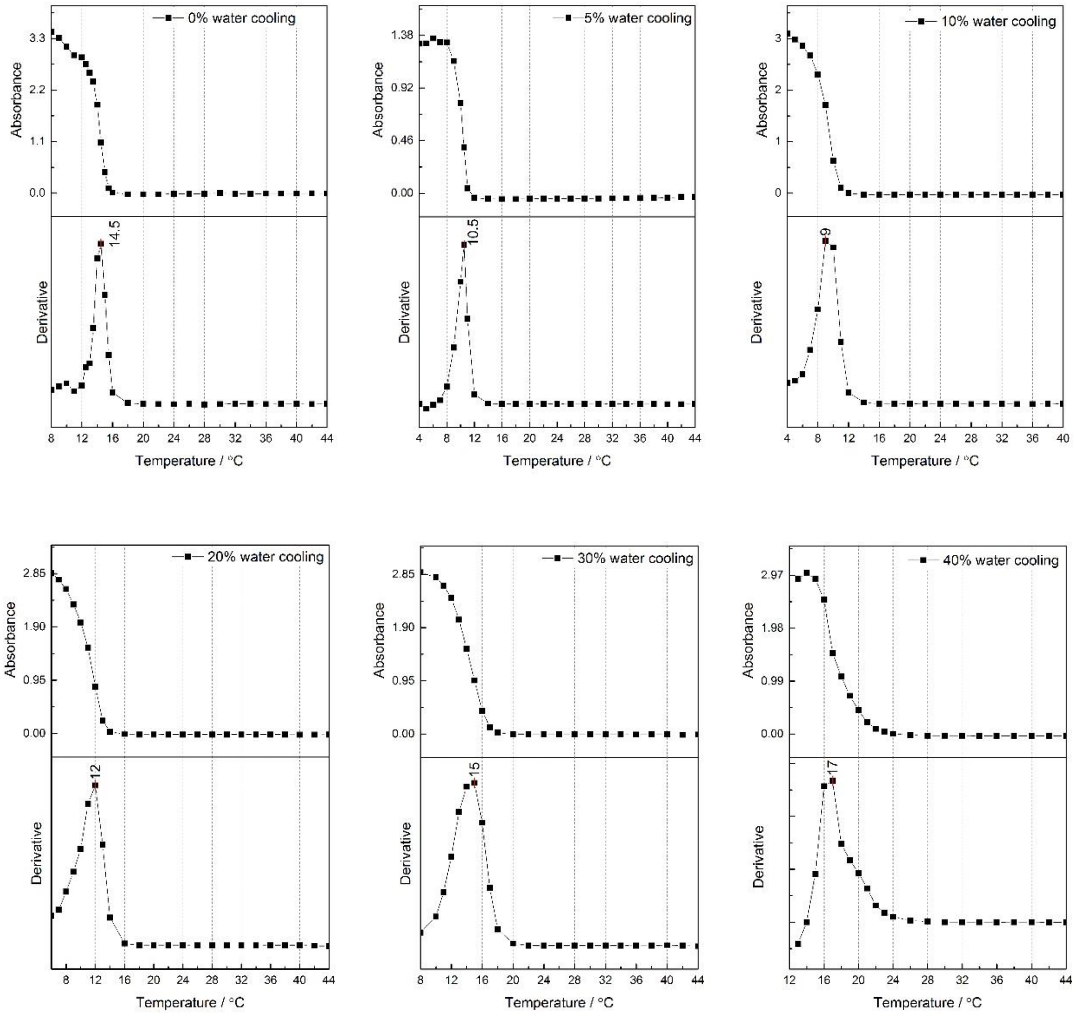

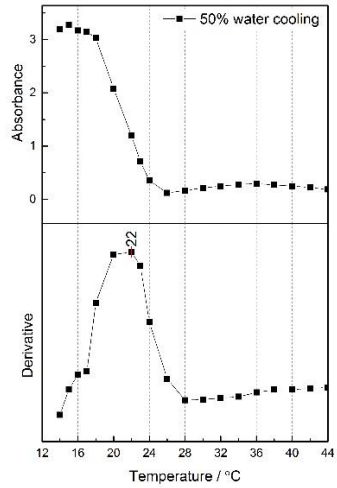

Fig.12. Absorbance as well as the derivative as a function of temperature for PEO-b-PCL block copolymer in different water-ethanol solvent mixtures, the maximum of the derivative is taken as the cloud points of the polymer solution upon cooling.

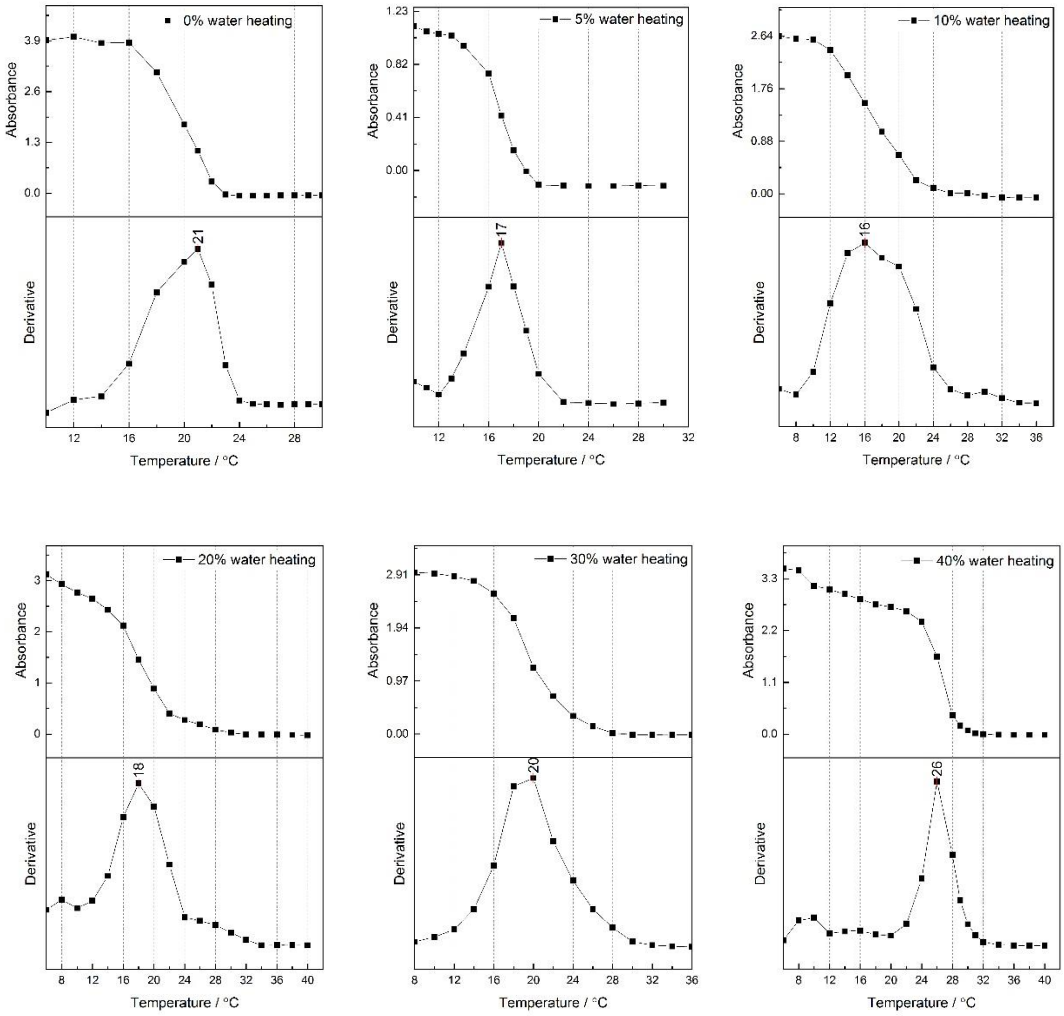

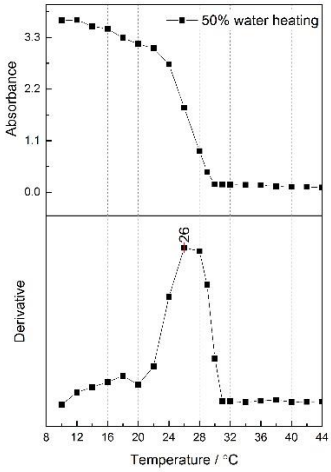

Fig.13. Absorbance as well as the derivative as a function of temperature for PEO-b-PCL block copolymer in different water-ethanol solvent mixtures, the maximum of the derivative is taken as the cloud points of the polymer solution upon heating.

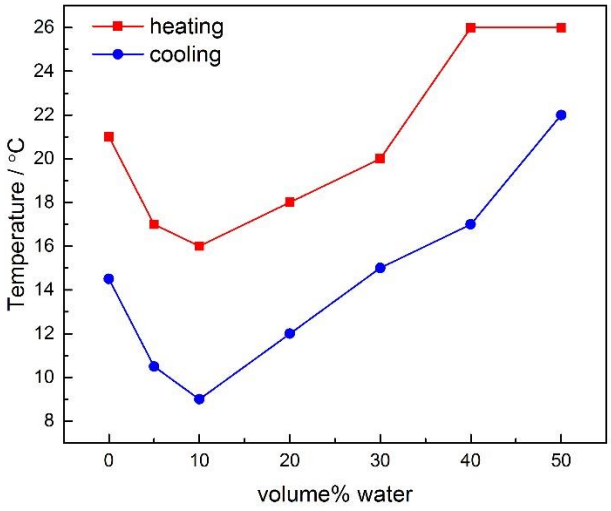

Fig.14. The obtained cloud points as a function of vol% of water upon cooling and heating.

The results of DSC measurements combined with cloud point measurements for PEO-b-PCL block copolymer in different solvent mixtures were shown in Fig.15 and relative temperature and enthalpies are listed in Table5. During cooling process, the crystallization of PEO-b-PCL block copolymer occurs right after the phase separation (the cloud points were marked with blue dots). Similar results can be obtained in heating process that after the crystal melts, a phase transition occurs, and the polymer become soluble afterwards. Moreover, the exothermic peaks are more obvious than the endothermic peaks, especially when the water content is above 20%. The reason could be the partial crystalline PEO-b-PCL that from thermal history has a different degree of crystallinity than cooling from the melted state. Besides, the mechanism of crystallization and

melting of PEO-b-PCL block copolymer is different.

In the DSC measurement, the peak area refers to the enthalpy changes during heating or cooling process, from which the crystallization energy per monomer can be calculated via:

$$\boldsymbol{E_{monomer}} = \frac{\boldsymbol{M}\ (g/mol) * \boldsymbol{E}(J/g)}{\boldsymbol{N_{AV}}(mol^{-1}) * \boldsymbol{n_u}(units)} \quad (18)$$

The crystallization energy per monomer for PEO (M=2000, n_u=44) and PCL (M=2000, n_u=17) homopolymers can be calculated as well as the average energy per monomer through: $\boldsymbol{E_{average}} = \frac{44 * E^{PEO} + 17 * E^{PCL}}{44+17}$. The effect of water addition on the crystallization energy per monomer is described in Fig.16, which shows the same trend in DSC results that the crystallization of PCL is not affected by adding water, but the crystallization energy of PEO decreases dramatically when more water is added and become almost zero. For PEO-b-PCL block copolymer in less than 20% water content solvent mixtures, the calculation under three possibilities can be done, by considering only PEO (M=2000, n_u=44) block crystallizes or only PCL (M=1400, n_u=12) block crystallizes or both PEO and PCL blocks (M=3400, n_u =56) crystallize. By comparing the crystallization energy per monomer of homopolymers with copolymer, the information of how each single block contributes to the crystallization of copolymer can be obtained. In Fig.17, the crystallization energy per monomer for both blocks crystallize is quite close to the average energy value, which indicates that both PEO and PCL blocks crystallize when a small amount water is added (less than 20% water).

Table5. DSC derived thermal data of PEO-b-PCL block copolymer in different solvent mixtures.

Samples	$\boldsymbol{T_c}$(℃)	$\boldsymbol{T_m}$(℃)	$\Delta \boldsymbol{H_{cooling}}(J/g)$
PEO-b-PCL (0vol%)	4.8	16.2	129.6
PEO-b-PCL (1vol%)	-5.3	7.8	113.6
PEO-b-PCL (5vol%)	-18.1	-1.7	98
PEO-b-PCL (10vol%)	-29	-6.5	74.2
PEO-b-PCL (20vol%)	-51	-21	19.5
PEO-b-PCL (30vol%)	13.4	5.03	3.7
PEO-b-PCL (40vol%)	14.8	10.8	10.4
PEO-b-PCL (50vol%)	13.5	17.2	14.7

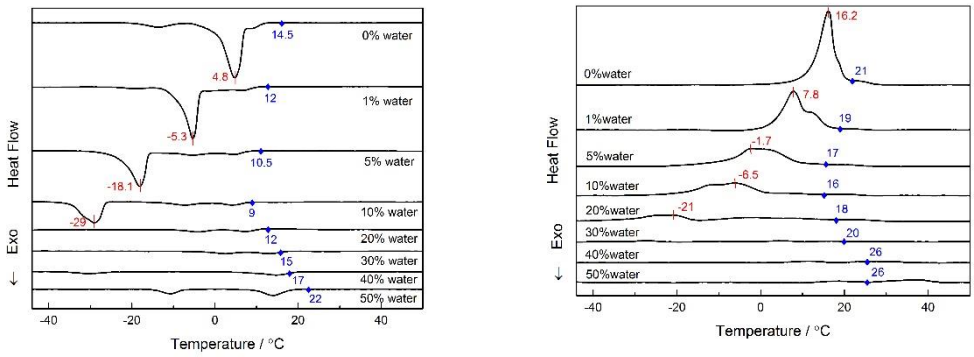

Fig.15. DSC cooling (left) and heating (right) scans of PEO-b-PCL block copolymer in different solvent mixtures, combined with the cloud point results (blue marks).

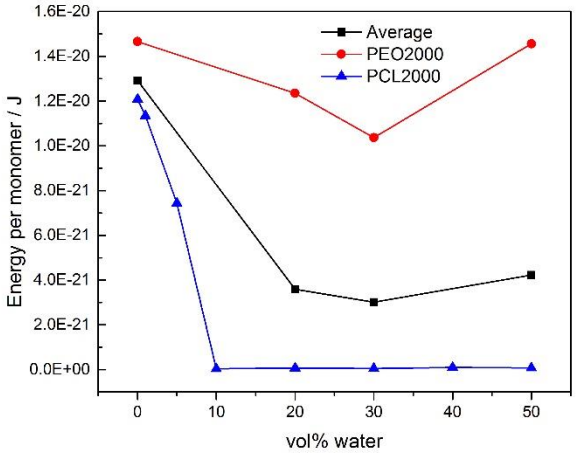

Fig.16. Crystallization energy per monomer for PEO and PCL homopolymers and the average value as a function of vol% of water.

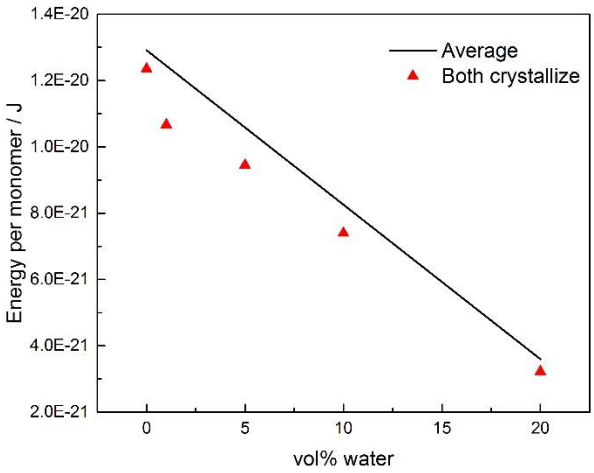

Fig.17. Comparison of crystallization energy per monomer of both blocks crystallize in copolymer with the average energy per monomer calculated from the homopolymers.

By combining the DSC and cloud point measurements, two phase diagrams of PEO-b-PCL block copolymer in water-ethanol solvent mixtures can be built upon cooling and heating (Fig.18). PEO-b-PCL block copolymer starts to crystallize (red line) after the phase separation (blue line) occurs, and both PEO and PCL blocks crystallize. With increasing amount of water in the system the crystallization behavior of PEO-b-PCL changes, occuring at higher temperature. The crystallization peaks appear just slightly below the phase separation temperature. The unknown transitions obtained by DSC (yellow and black dash line) may be associated with structural rearrangement of the copolymer chains. Even though the transitions occur during both heating and cooling process, cooling process provides more distinguished transitions.

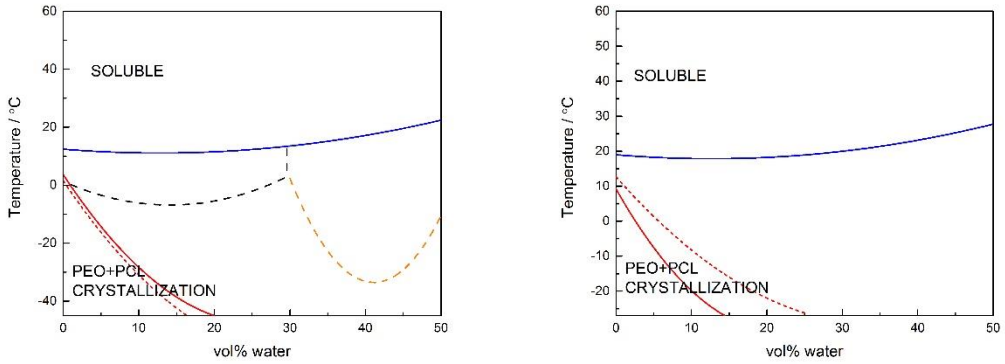

Fig.18. Phase diagrams derived from DSC and cloud point measurement upon cooling (left) and heating (right). Red solid lines are the onset temperature of crystallization and red dash lines are the maximum crystallization temperature. Blue lines are the phase separation temperature. Yellow and black dash lines represent the unknown peaks and transitions in DSC.

To further understand the structure of PEO-b-PCL block copolymer in each phases, SAXS and WAXS measurements were carried out in pure ethanol and 50% water-ethanol mixtures. The WAXS profiles for PEO and PCL homopolymers in ethanol, 50%water-ethanol mixtures and in bulk were also measured as a reference (Fig.19). PCL homopolymer in bulk shows three diffraction peaks at d-spacing of 3.61Å, 3.26 Å and 2.67 Å respectively. In both ethanol and water-ethanol mixtures, two main peaks (at 3.61Å and 3.26 Å) can still be observed, showing in agreement with the DSC results, that the PCL homopolymer crystallize in both conditions. The presence of a new diffraction peak appears at 2.95 Å in ethanol and the disappearance of 2.67 Å in water-ethanol mixtures may be related to a change in crystallization mechanism, associated with the presence of the solvent molecules. This means even though the solvent environments do not hinder the crystallization of PCL, but indeed change the arrangement of PCL chains during crystallization.

In the case of PEO, diffraction peaks at 3.31 Å and 4.01 Å remain in the same position in ethanol, but totally vanish in 50%water content, in a good agreement with the DSC results and implies that

PEO become soluble with the addition of water, which prevents PEO from crystallizing. The multiple diffraction peaks that present in bulk state might related to different orientation of PEO crystal due to the absorbed water molecules.

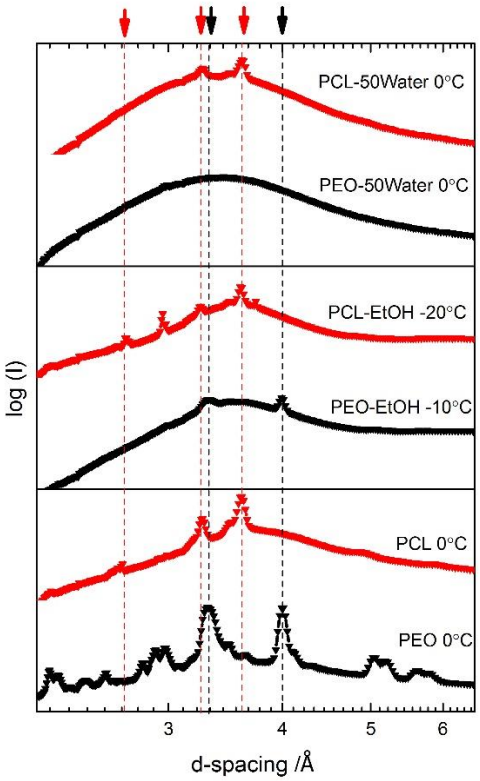

Fig.19. WAXS patterns at indicated temperatures and solvent composition for PEO2000 (black) and PCL2000 (red) homopolymers.

WAXS for PEO-b-PCL block copolymer in ethanol at different temperatures has been measured upon cooling and heating (Fig.20). During the heating process, at -20℃ and 15℃ three diffraction peaks can be found at 4.01 Å, 3.61 Å and 3.31 Å, which corresponds to the PEO diffraction peak, PCL diffraction peak and the overlap of PEO and PCL diffraction peak respectively. This indicates PEO and PCL blocks co-crystallize together in ethanol, which confirms what derived from the estimation of crystallization energies per monomer. At 40℃ the crystal melt and the diffraction peaks disappear. Similar results can be obtained upon cooling. In Fig.21 it is shown that in 50% water-ethanol mixtures the diffraction peaks of PEO-b-PCL block copolymer (at 3.26 Å and 3.61 Å) comes only from the crystallization of PCL block. As discussed, PEO block does not crystallize at high water content, due to the good solvency of water for PEO.

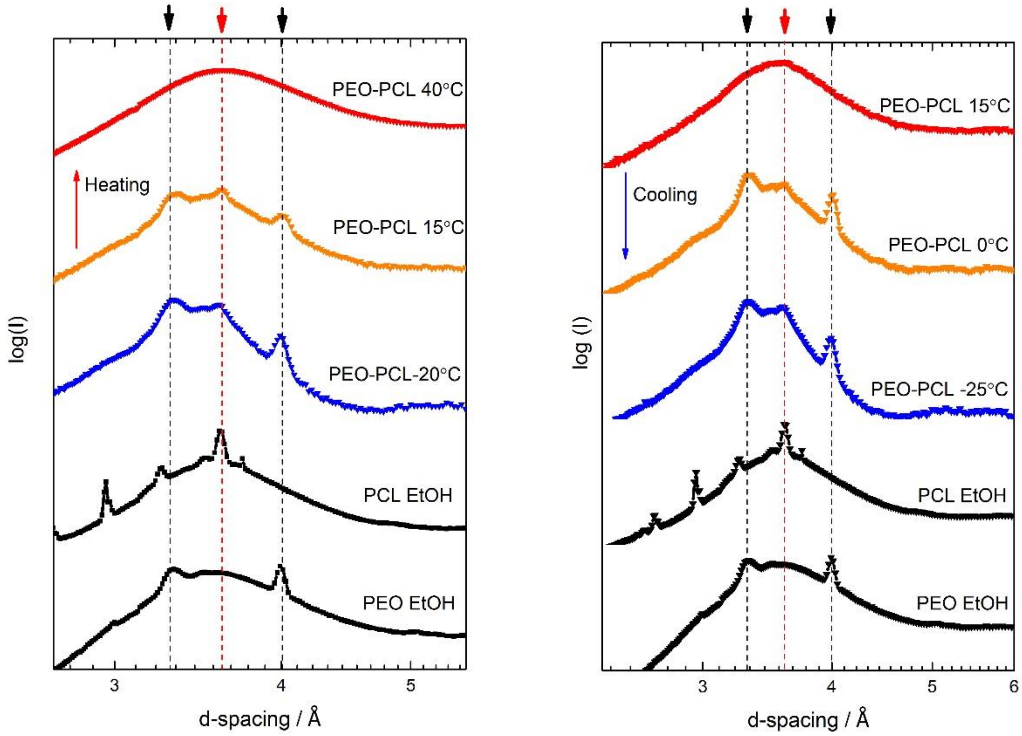

Fig.20. WAXS pattern at the indicated temperatures in ethanol solvent for PEO-b-PCL block copolymer upon cooling and heating. (PEO and PCL homopolymers are shown in the bottom as a reference)

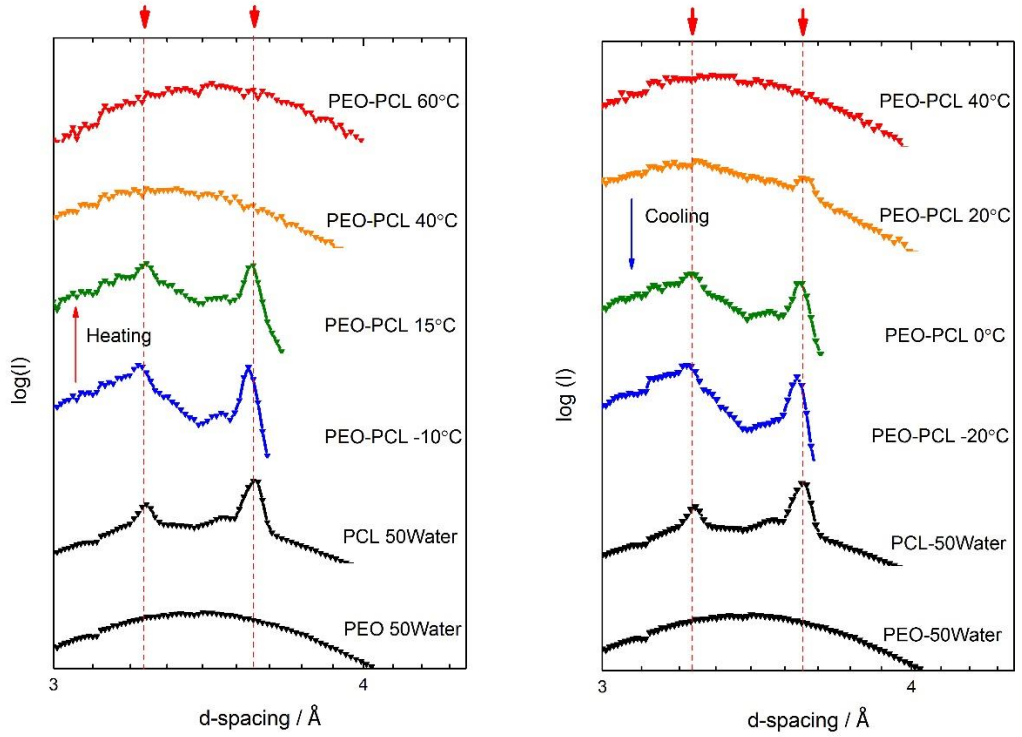

Fig.21. WAXS patterns at the indicated temperatures in 50% water-ethanol solvent mixtures for

PEO-b-PCL block copolymer upon cooling and heating. (PEO and PCL homopolymers are shown in the bottom as a reference)

To understand the aggregation behavior of PEO-b-PCL block copolymer in ethanol and water-ethanol mixtures, SAXS experiments were performed at different temperatures. Fig.22 shows the SAXS patterns obtained in ethanol upon cooling and heating. At low temperature the presence of diffraction peaks in the SAXS region indicates the presence on an internal long-range ordering, associated with the segregation of the two blocks (nano-phase separation). The ratio of each peak position relative to the first peak provides the information of the morphology, which can be checked from Table 3. At -20℃ (upon heating), the ratio of 1: $\sqrt{2}$: 2: 3 indicates a mixed morphology of body-centered-cubic (BCC) and lamellar phases. Increasing the temperature to 15℃ the first peak shift to lower q value and the peak ratio of 1: $\sqrt{2}$: $\sqrt{3}$ indicates the presence of a BCC phase only. Similar morphology transition can be found upon cooling: only BCC phase is obtained at 0℃ and the coexistence of BCC and lamellar symmetry appears at -25℃. Therefore, temperature can be used as a tuning parameter for controlling the phase symmetry of the nano-phase separated domains, which are formed after the macroscopic phase separation in ethanol.

At higher temperature, 40 ℃ (upon heating) and 15 ℃ (upon cooling), the peaks disappear thoroughly. However, the SAXS profiles can be well fitted with the form factor of a polymer coil with excluded volume, where the scattered intensity scales as $q^{5/3}$ (Fig.23). This means that at higher temperature the polymer become completely soluble and exist as individual polymer coils in solution. From the form factor fitting the radius of gyration of the polymer, $R_g = 2.3$nm has been obtained. Therefore, the ratio $R_h/R_g = 0.65$ is calculated (the hydrodynamic radius $R_h \approx 1.5$nm is obtained from DLS (Table6)), which is the typical value for polymer coils in solution[53] and further confirms the presence of polymer coils.

When the temperature is decreased up to 15℃ (Fig.23(b)), close to the demixing temperature, an increase in intensity appears in the low q range (Fig.23(a)). This deviation is associated with a contribution of the structure factor and indicates the tendency to aggregate of polymer coils due to the decreased quality of the solvent.

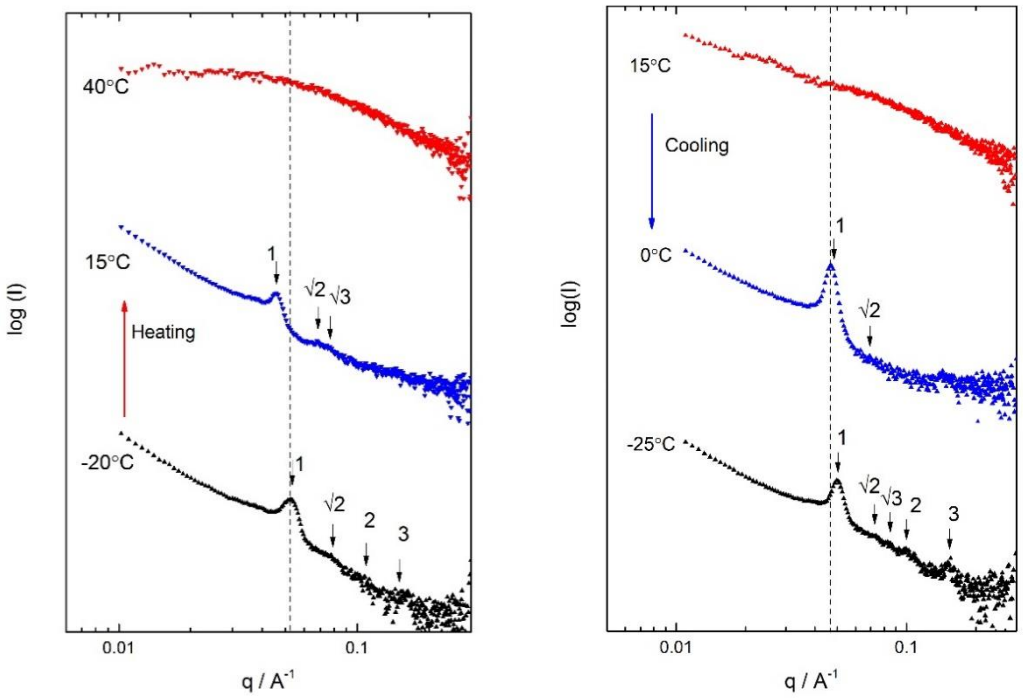

Fig.22. SAXS patterns at the indicated temperatures in ethanol for PEO-b-PCL block copolymer upon cooling and heating.

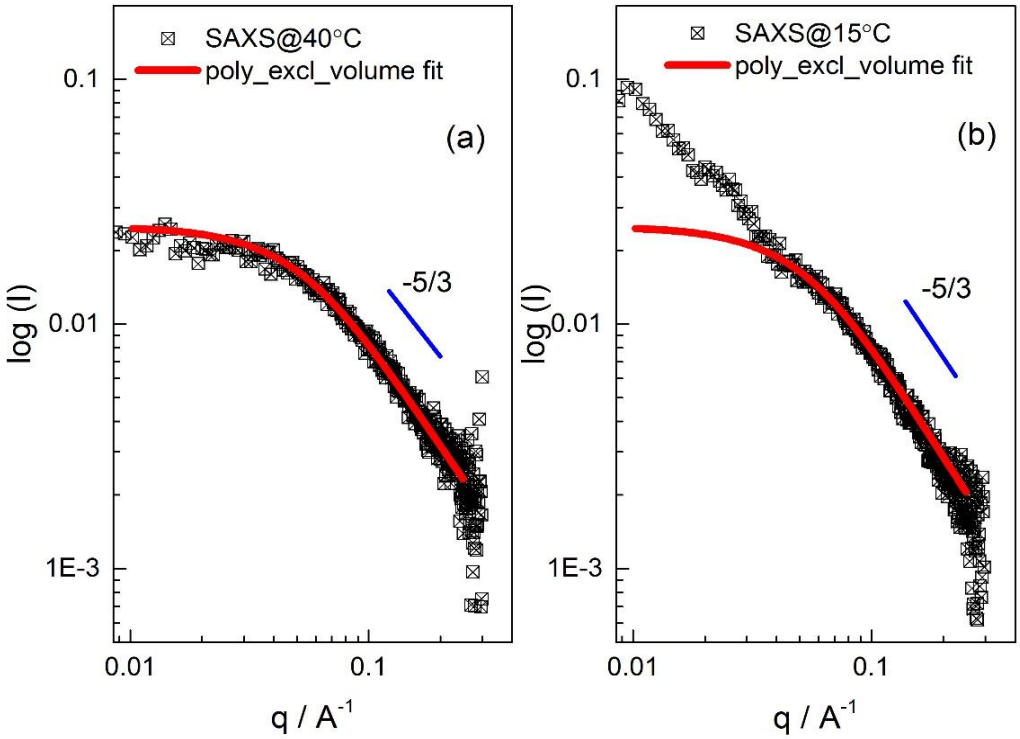

Fig.23. SAXS profiles collected at 40℃ and 15℃ for PEO-b-PCL block copolymer in ethanol. The SAXS data (hollow square) were fitted with a polymer coil with excluded volume model (red lines).

The SAXS pattern of PEO-b-PCL block copolymer in 50% water-ethanol mixtures were obtained at different temperatures (Fig.24). At high temperature (60℃) the scattered intensity barely change through the entire q range. A possible explanation could be that the particles formed are much bigger than the probed length scale. In the cooling process, a face-centered-cubic (FCC) phase is obtained at 20℃ and 0℃ with peak ratio of 1: $\sqrt{3}$: $\sqrt{8}$: 3. This is produced by the nano-phase separation which is induced by lowering the temperature. Comparing with the behavior of polymer in pure ethanol, we can conclude that the addition of water also causes a morphological transition in the aggregate.

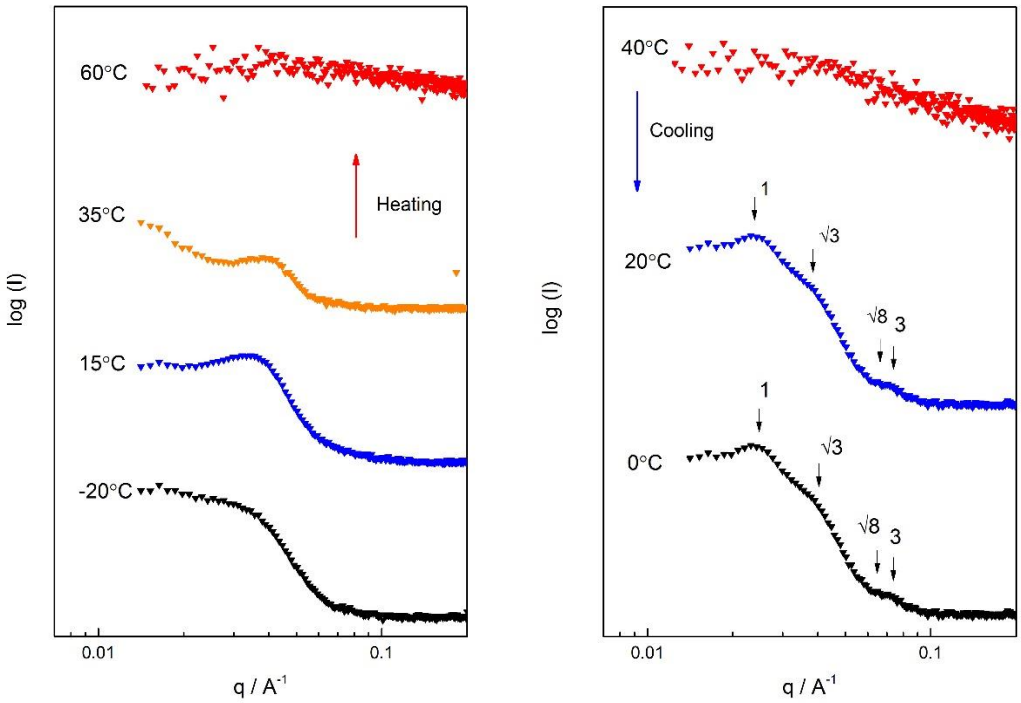

Fig.24. SAXS patterns at the indicated temperatures in 50% water-ethanol for PEO-b-PCL block copolymer upon cooling and heating.

Dynamic light scattering and static light scattering were measured to study the morphology and the size of PEO-b-PCL block copolymer in 20 and 30% mixtures at temperature higher than the (apparent) cloud points. The diffusion coefficient D was obtained from the relation $\Gamma = q^2 D$ with Γ being the decay rate of the autocorrelation function. Following, the hydrodynamic radius R_h was calculated via Stoke-Einstein equation (Table6). In all measurements two different relaxation times can be observed at each temperature, the fast one associated with the motion of free polymer molecules (with $R_h \approx 1.5$nm, Fig.25(b) and Fig.26(b)) and slow one associated with aggregates (having $R_h \approx 200$nm in 20% and $R_h \approx 75$nm in 30% water-ethanol mixtures, Fig.25(a) and Fig.26(a)). The hydrodynamic size of the assemblies increases with decreasing the temperature. This could be caused by an increasing aggregation number of the assemblies, associated with a

decrease in solubility of the copolymer molecules.

At high q, the fractal dimension of the objects can be obtained from the slope of $\log R_\theta$ vs $\log q$ plot (Fig.27), which provides information on the possible morphologies of PEO-b-PCL assemblies present in solution. At 20% water-ethanol solvent mixtures, vesicles or disk-shaped structures might be formed, as testified by a fractal dimension around 2 (Fig.27(a)). However, at 30% water-ethanol mixtures, the fractal dimension of 1 (Fig.27(b)) shows a possible presence of cylindrical structures. This indicates the possibility of tuning the morphology and size of the PEO-b-PCL assemblies by simply tuning the solvent composition, in agreement with the finding of A. Eisenberg and coworkers[20]. However, this morphological transition is yet to be confirmed with other experimental techniques.

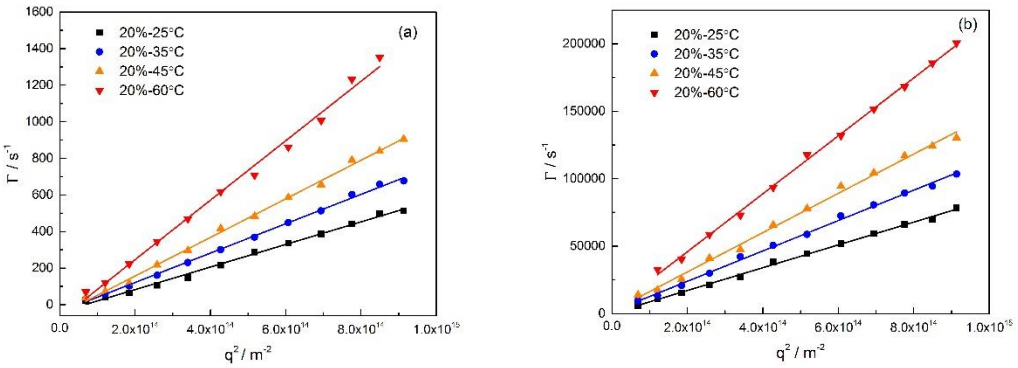

Fig.25. The decay rate Γ vs q^2 of PEO-b-PCL block copolymer in 20% water-ethanol solvent mixtures at indicated temperatures.

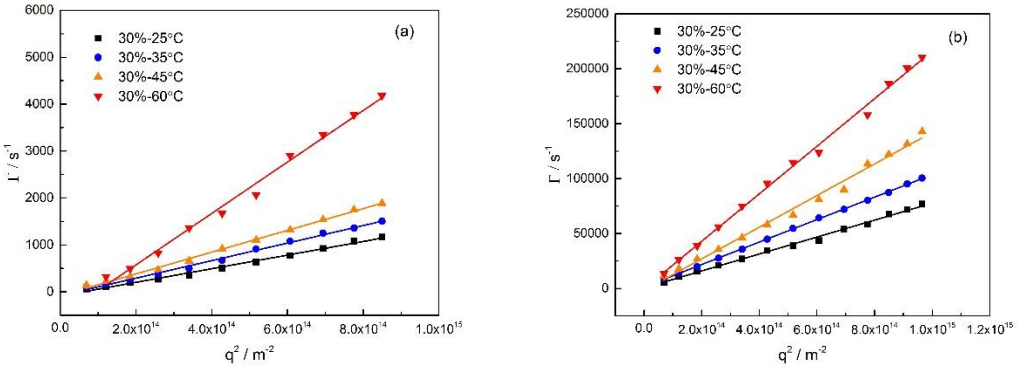

Fig.26. The decay rate Γ vs q^2 of PEO-b-PCL block copolymer in 30% water-ethanol solvent mixtures at indicated temperatures.

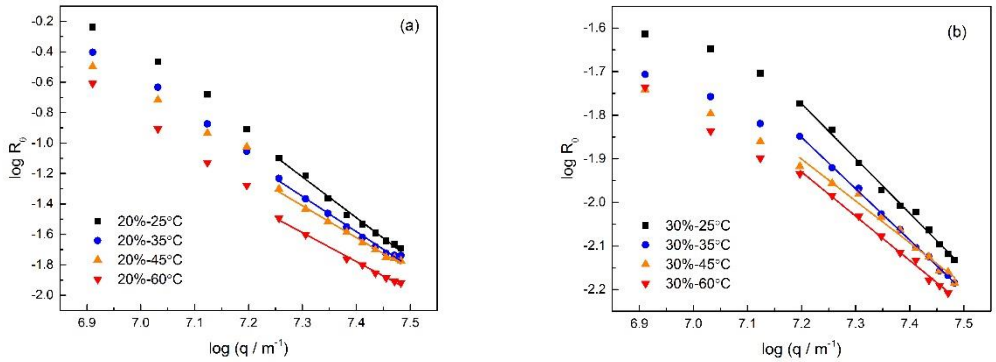

Fig.27. The light scattering profile for PEO-b-PCL block copolymer in 20% (a) and 30% (b) water-ethanol mixtures at indicated temperature.

Table6. The derived results from SLS and DLS measurements for PEO-b-PCL block copolymer in 20% and 30% water-ethanol solvent mixtures.

Samples	Diffusion coefficient (m^2/s)		R_h (nm)		d_f
30%water-60℃	5.48E-12	2.16E-10	52	1.32	1.06
30%water-45℃	2.48E-12	1.44E-10	77.5	1.34	1.11
30%water-35℃	1.86E-12	1.02E-10	77.7	1.42	1.21
30%water-25℃	1.45E-12	7.71E-11	79.2	1.42	1.21
20%water-60℃	1.62E-12	2.16E-10	190	1.43	1.87
20%water-45℃	1.05E-12	1.45E-10	204	1.48	2.04
20%water-35℃	8.03E-13	1.11E-10	206	1.49	2.33
20%water-25℃	6.17E-13	8.44E-11	207	1.52	2.38

Combing all the results from scattering studies, the phase diagram of polymer solution can be further completed, with focus on the behavior of the system upon cooling (Fig.28). At high temperature PEO-b-PCL block polymers are soluble in ethanol and exist as polymer coils. Then marco-phase separation occurs when lowering the temperature, followed by a micro-phase separation into BCC symmetry. Further decrease the temperature both PEO and PCL blocks will crystallize into lamellar morphology with coexist with BCC symmetry. By adding water in the system, polymers tend to self-assemble into different morphologies (20% for vesicles and 30% for cylinders) due to the poor solvency of water. When more water is added (50% water content) a morphological transition from BCC to FCC symmetry is observed below the cloud points, where only PCL block crystallize.

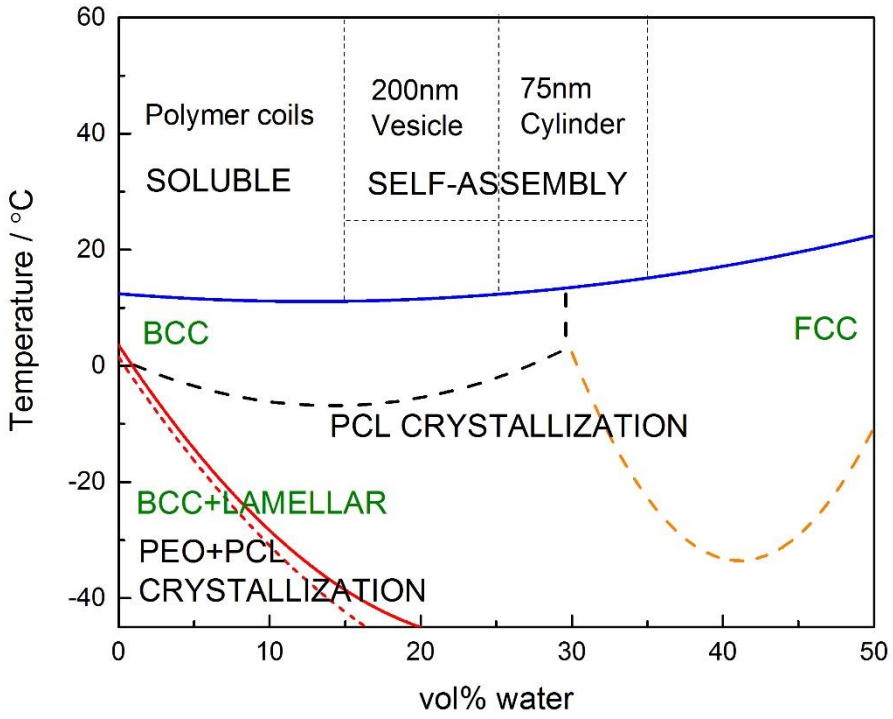

Fig.28. Phase diagram of PEO-b-PCL derived from DSC, WAXS, SAXS, light scattering and cloud point measurements based on cooling process.

However, as shown in the phase diagram, at 50% water-ethanol mixtures the self-assembly of PEO-b-PCL at room temperature is hindered by the crystallization that occurs right after the phase separation.

3.3 Use of additives to prevent the crystallization of the PEO-b-PCL block copolymers

Since the crystallization affect the self-assembly behavior, we explore the possibility of preventing or reducing the crystallization of the block copolymer by means of additives. Acetyl tributyl citrate (ATBC) is chosen as an additive in the polymer solution. ATBC has been reported as a biodegradable plasticizer for PEO/PCL-blended film, leading to the decrease of crystallinity and glass transition temperature[54]. Therefore, DSC measurement was carried out to study the thermal behavior of PEO-b-PCL block copolymer in solvent mixtures after adding ATBC.

Fig. 29(a) shows that the present of ATBC barely change the crystallization temperature and melting

temperature of PEO-b-PCL in ethanol solvent, and the enthalpies also remain roughly the same after adding ATBC. This implies ATBC cannot penetrate into the folded chains because both PEO and PCL blocks crystallize and are compact packed. However, when ATBC is added in the 50% water-ethanol solvent mixtures, the thermal behavior changes as shown in Fig.29(b). Both T_c and T_m shift to lower value and overlap with the polymer chains rearrangement transition temperature. At 50% water-ethanol mixtures only PCL block crystallize, and the PEO block become solvated which allows ATBC to penetrate into the PCL region. Due to the polar interactions between the ester groups of ATBC and PCL, the interaction between the polymer chain decreases and the free volume increases, which therefore influences the T_c and T_m of PEO-b-PCL block copolymer[54]. Even though the crystallization of the polymer become easier with the presence of additive, the crystallization temperature indeed decreases in a large extent, which is desired in our system. This reduction of temperatures can be found also for PCL homopolymer in 50% water-ethanol mixtures (Fig.29(c) and Table7), which indicates the interaction between ATBC and PCL block plays an essential role in the reduction of T_c and T_m of PEO-b-PCL block copolymer.

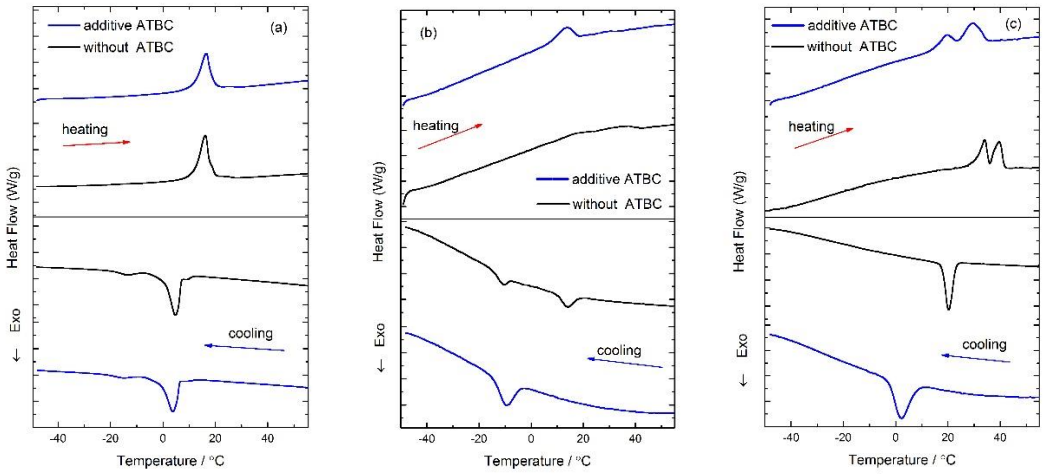

Fig.29. DSC cooling and heating scan of PEO-b-PCL block copolymer with or without additive ATBC in pure ethanol (a), in 50% water-ethanol solvent mixtures (b), and PCL homopolymer in 50% water-ethanol solvent mixtures (c).

Table7. DSC derived thermal data of PEO-b-PCL block copolymer and PCL homopolymer in pure ethanol and 50% water-ethanol solvent mixtures.

Samples	T_m(℃)	T_c(℃)	$\Delta H_{cooling}$(J/g)
PEO-b-PCL-EtOH	16.2	4.8	124.8
PEO-b-PCL-EtOH-ATBC	16.55	3.84	118.6
PEO-b-PCL-50%Water	36.6	13.5	14.7
PEO-b-PCL-50%Water-ATBC	15.2	-8.72	31.65

PCL-50%Water	34.1	39	20.4	76.7
PCL-50%Water-ATBC	19.5	29.4	2.13	76.6

4. Conclusions and outlook

We have studied the complex behavior of PEO-b-PCL block copolymers in different water-ethanol solvent mixtures. Based on different characterization methods, it has been shown that the PEO-b-PCL block copolymers experienced self-assembly, phase separation and crystallization in solution which compete and induce each other. Since ethanol is a poorly selective solvent and water is a highly selective solvent for PEO-b-PCL, the self-assembly structures can be possible tuned in the water-ethanol mixtures by changing the solvent composition. Moreover, due to the UCST behavior of PEO-b-PCL in ethanol, the stability of polymer solution can be controlled by temperature. Therefore, the morphological transitions of polymer were achieved under different temperature condition. The results of phase behavior, thermal behavior and self-assembly studies of PEO-b-PCL are summarized here.

In pure ethanol, PEO-b-PCL exist as polymer coils at high temperature. By increasing the water content to 20%, vesicles with radius of 200nm are formed and the self-assembled cylinder micelles are obtained at 30% water content. The behavior of the system at 50% water content is still under study. We used an additive, acetyl tributyl citrate to control the crystallization temperature of polymer in order to gain more control on the assembly process. The presence of the additive increases the crystallinity of the polymer but drastically reduces the crystallization temperature.

Due to the UCST behavior of PEO-b-PCL in ethanol, phase separation of polymer solution occurs by lowering the temperature. The nano-phase separation follows immediately with the formation of body-centered-cubic (BCC) phase. Upon further decreasing of the temperature both PCL and PEO blocks crystallize into lamellar crystal. The lamellar phase coexists with the BCC phase. A morphological transition in bulk can be induced by changing temperature as well as solvent composition. A face-centered-cubic (FCC) phase is obtained after phase separation by adding water until 50%. Moreover, the addition of water over 30% prevent the crystallization of PEO block.

A thermoresponsive PEO-b-PCL block copolymer has been explored in water-ethanol solvent mixtures in our study, and the morphological transition and phase behavior of the polymer solution have been achieved by tuning the solvent composition as well as the temperature. This work provided a possible new strategy for designing smart material in nanomedical field.

For future understanding, the morphology of PEO-b-PCL in water-ethanol solvent mixtures needed to be studied in detail with the combination of microscopic techniques, such as cryo-electron microscopy (cryo-EM) and atomic force microscopy (AFM). To fully understand the mechanism of the morphological transition in behind, scattering techniques with higher resolution are required as well as the theoretical supports.

Reference

[1] A. Pitto-Barry and N. P. E. Barry, "Pluronic® block-copolymers in medicine: from chemical and biological versatility to rationalisation and clinical advances," *Polym. Chem*, vol. 5, no. 10, pp. 3291–3297, 2014.

[2] M. Ramanathan, L. K. Shrestha, T. Mori, Q. Ji, J. P. Hill, and K. Ariga, "Amphiphile nanoarchitectonics: from basic physical chemistry to advanced applications," *Phys. Chem. Chem. Phys.*, vol. 15, no. 26, pp. 10580–10611, 2013.

[3] A. Rösler, G. W. M. Vandermeulen, and H. A. Klok, "Advanced drug delivery devices via self-assembly of amphiphilic block copolymers.," *Adv. Drug Deliv. Rev.*, vol. 53, no. 1, pp. 95–108, 2001.

[4] G. Riess, "Micellization of block copolymers," *Prog. Polym. Sci.*, vol. 28, no. 7, pp. 1107–1170, 2003.

[5] J.K.stille, "Step-Growth Polymerization," *J. Chem. Educ.*, vol. 58, no. 11, pp. 862–866, 1981.

[6] B. Bonillo and T. M. Swager, "Chain-growth polymerization of 2-chlorothiophenes promoted by lewis acids," *J. Am. Chem. Soc.*, vol. 134, no. 46, pp. 18916–18919, 2012.

[7] O. Nuyken and S. D. Pask, "Ring-opening polymerization-An introductory review," *Polymers (Basel).*, vol. 5, no. 2, pp. 361–403, 2013.

[8] K. M. Stridsberg, M. Ryner, and A.-C. Albertsson, "Controlled Ring-Opening Polymerization: Polymers with designed Macromolecular Architecture," *Degrad. Aliphatic Polyesters*, vol. 157, pp. 41–65, 2002.

[9] E. Goethals, A. C. Albertsson, and I. K.Varma, "Aliphatic Polyesters: synthesis, properties and applications," in *Advances in Polymer Science*, A.C.Albertsson, Ed. Springer, 1977, pp. 7–15.

[10] H. MORINAGA, BUNGO OCHIAI, and T. ENDO, "Synthesis and Properties of Star-Shaped Polymers by the Ring-Opening Polymerization of Cyclic Carbonate Initiated with a Trifunctional, Poly(ethylene glycol)-Based Surfactant," *J. Polym. Sci. part A Polym. Chem.*, vol. 44, pp. 6633–6639, 2006.

[11] H. Feng, X. Lu, W. Wang, N.-G. Kang, and J. Mays, "Block Copolymers: Synthesis, Self-Assembly, and Applications," *Polymers (Basel).*, vol. 9, no. 10, pp. 494–525, 2017.

[12] F. S. Bates and G. H. Fredrickson, "Block Copolymers — Designer soft materials," *Phys. Today*, vol. 2, no. 52, pp. 32–38, 1999.

[13] Y. Mai and A. Eisenberg, "Self-assembly of block copolymers," *Chem. Soc. Rev.*, vol. 41, no. 18, pp. 5969–5985, 2012.

[14] A. Ianiro *et al.*, "A roadmap for poly(ethylene oxide)-block-poly-ε-caprolactone self-assembly in water: Prediction, synthesis, and characterization," *J. Polym. Sci. Part B Polym. Phys.*, vol. 56, no. 4, pp. 330–339, 2018.

[15] R. Nagarajan, "Molecular packing parameter and surfactant self-assembly: The neglected role of the surfactant tail," *Langmuir*, vol. 18, no. 1, pp. 31–38, 2002.

[16] J. N. Israelachvili, D. J. Mitchell, and B. W. Ninham, "Theory of self-assembly of hydrocarbon amphiphiles into micelles and bilayers," *J. Chem. Soc. Faraday Trans. 2*, vol. 72, pp. 1525–1568, 1976.

[17] T. Smart, H. Lomas, M. Massignani, M. V. Flores-Merino, L. R. Perez, and G. Battaglia, "Block copolymer nanostructures," *Nano Today*, vol. 3, no. 3–4, pp. 38–46, 2008.

[18] A. Blanazs, S. P. Armes, and A. J. Ryan, “Self-assembled block copolymer aggregates: From micelles to vesicles and their biological applications,” *Macromol. Rapid Commun.*, vol. 30, no. 4–5, pp. 267–277, 2009.

[19] H. Shen and A. Eisenberg, “Morphological Phase Diagram for a Ternary System of Block Copolymer PS $_{310}$ - *b* -PAA $_{52}$ /Dioxane/H $_{2}$ O,” *J. Phys. Chem. B*, vol. 103, no. 44, pp. 9473–9487, 1999.

[20] A. Choucair and A. Eisenberg, “Control of amphiphilic block copolymer morphologies using solution conditions,” *Eur. Phys. J. E*, vol. 10, no. 1, pp. 37–44, 2003.

[21] S. Qin, Y. Geng, D. E. Discher, and S. Yang, “Temperature-controlled assembly and release from polymer vesicles of poly(ethylene oxide)-block-poly(N-isopropylacrylamide),” *Adv. Mater.*, vol. 18, no. 21, pp. 2905–2909, 2006.

[22] P. Bhargava, Y. Tu, J. X. Zheng, H. Xiong, R. P. Quirk, and S. Z. D. Cheng, “Temperature-induced reversible morphological changes of polystyrene-block-poly(ethylene oxide) micelles in solution,” *J. Am. Chem. Soc.*, vol. 129, no. 5, pp. 1113–1121, 2007.

[23] A. Can, S. Hoeppener, P. Guillet, J. F. Gohy, R. Hoogenboom, and U. S. Schubert, “Upper Critical Solution Temperature Switchable Micelles Based on Polystyrene-block-poly(methyl acrylate) Block Copolymers,” *J. Polym. Sci. part A Polym. Chem.*, vol. 49, pp. 3681–3687, 2011.

[24] P. J. Roth, T. P. Davis, and A. B. Lowe, “UCST-driven self-assembly and crosslinking of diblock copolymer micelles,” *Polym. Chem.*, vol. 3, no. 8, pp. 2228–2235, 2012.

[25] M. L. Huggins, “Theory of Solutions of High Polymers,” *J. Am. Chem. Soc.*, vol. 64, no. 7, pp. 1712–1719, 1942.

[26] A. Gandhi, A. Paul, S. O. Sen, and K. K. Sen, “Studies on thermoresponsive polymers: Phase behaviour, drug delivery and biomedical applications,” *Asian J. Pharm. Sci.*, vol. 10, no. 2, pp. 99–107, 2015.

[27] Q. Zhang, C. Weber, U. S. Schubert, and R. Hoogenboom, “Thermoresponsive polymers with lower critical solution temperature: from fundamental aspects and measuring techniques to recommended turbidimetry conditions,” *Mater. Horiz.*, vol. 4, no. 2, pp. 109–116, 2017.

[28] Y. Zhang, S. Furyk, D. E. Bergbreiter, and P. S. Cremer, “Specific ion effects on the water solubility of macromolecules: PNIPAM and the Hofmeister series,” *J. Am. Chem. Soc.*, vol. 127, no. 41, pp. 14505–14510, 2005.

[29] W. Zhang, N. Ning, Y. Gao, F. Xu, and Q. Fu, “Stretching induced interfacial crystallization and property enhancement of poly(l-lactide)/single-walled carbon nanotubes fibers,” *Compos. Sci. Technol.*, vol. 83, pp. 47–53, 2013.

[30] L. Li, W. Wang, E. D. Laird, C. Y. Li, M. Defaux, and D. A. Ivanov, “Polyethylene/carbon nanotube nano hybrid shish-kebab obtained by solvent evaporation and thin-film crystallization,” *Polymer (Guildf).*, vol. 52, no. 16, pp. 3633–3638, 2011.

[31] A. J. Müller, V. Balsamo, and M. L. Arnal, “Nucleation and crystallization in diblock and triblock copolymers,” *Adv. Polym. Sci.*, vol. 190, no. 1, pp. 1–63, 2005.

[32] T. Yu *et al.*, “Solution crystallization behavior of linear and star-shaped poly(ethylene glycol)-b-poly(elipson-caprolactone) block copolymers,” *Chinese J. Polym. Sci. (English Ed.*, vol. 31, no. 12, pp. 1717–1724, 2013.

[33] S. Nojima, M. Toei, S. Hara, S. Tanimoto, and S. Sasaki, “Size dependence of crystallization within spherical microdomain structures,” *Polymer (Guildf).*, vol. 43, no. 14, pp. 4087–4090, 2002.

[34] K. Knop, R. Hoogenboom, D. Fischer, and U. S. Schubert, “Poly(ethylene glycol) in drug delivery: Pros and cons as well as potential alternatives,” *Angew. Chemie - Int. Ed.*, vol. 49, no. 36, pp. 6288–6308, 2010.

[35] S. Saeki, N. Kuwahara, M. Nakata, and M. Kaneko, “Upper and lower critical solution temperatures in poly (ethylene glycol) solutions,” *Polymer (Guildf).*, vol. 17, no. 8, pp. 685–689, 1976.

[36] S. Y. Oh and Y. C. Bae, “Closed miscibility loop phase behavior of polymer solutions,” *Polymer (Guildf).*, vol. 49, no. 20, pp. 4469–4474, 2008.

[37] D. L. Ho, B. Hammouda, S. R. Kline, and W. R. Chen, “Unusual phase behavior in mixtures of poly(ethylene oxide) and ethyl alcohol,” *J. Polym. Sci. Part B Polym. Phys.*, vol. 44, no. 3, pp. 557–564, 2006.

[38] J. Sun, X. Chen, C. He, and X. Jing, “Morphology and structure of single crystals of poly(ethylene glycol)-poly(E-caprolactone) diblock copolymers,” *Macromolecules*, vol. 39, no. 11, pp. 3717–3719, 2006.

[39] L. G. . Beekmans and G. . Vancso, “Real-time crystallization study of poly(ϵ-caprolactone) by hot-stage atomic force microscopy,” *Polymer (Guildf).*, vol. 41, no. 25, pp. 8975–8981, 2000.

[40] M. L. Arnal, F. Lopez Carrasquero, E. Laredo, and A. J. Muller, “Coincident or sequential crystallization of PCL and PEO blocks within polystyrene-b-poly(ethylene oxide)-b-poly(??-caprolactone) linear triblock copolymers,” *Eur. Polym. J.*, vol. 40, no. 7, pp. 1461–1476, 2004.

[41] A. Ianiro, I. Jiménez-Pardo, A. C. C. Esteves, and R. Tuinier, “One-pot, solvent-free, metal-free synthesis and UCST-based purification of poly(ethylene oxide)/poly-ε-caprolactone block copolymers,” *J. Polym. Sci. Part A Polym. Chem.*, vol. 54, no. 18, pp. 2992–2999, 2016.

[42] R. M. Van Horn *et al.*, “Solution crystallization behavior of crystalline-crystalline diblock copolymers of poly(ethylene oxide)-block-poly(ε-caprolactone),” *Macromolecules*, vol. 43, no. 14, pp. 6113–6119, 2010.

[43] F. Xue and S. Jiang, “Crystallization behaviors and structure transitions of biocompatible and biodegradable diblock copolymers,” *Polymers (Basel).*, vol. 6, no. 8, pp. 2116–2145, 2014.

[44] C. He, J. Sun, C. Deng, T. Zhao, M. Deng, and X. Chen, “Study of the Synthesis , Crystallization , and Morphology of Poly (ethylene glycol) - Poly (E -caprolactone) Diblock Copolymers,” *Biomacromolecules*, vol. 5, no. 5, pp. 2042–2047, 2004.

[45] J. H. An, H. S. Kim, D. J. Chung, and D. S. Lee, “Thermal behaviour of poly (ε -caprolactone) - poly (ethylene glycol) -poly (ε -caprolactone) tri-block copolymers,” *J. Mater. Sci.*, vol. 36, pp. 715–722, 2001.

[46] Q. Zhang and R. Hoogenboom, “Polymers with upper critical solution temperature behavior in alcohol / water solvent mixtures,” *Prog. Polym. Sci.*, vol. 48, pp. 122–142, 2015.

[47] F.Franks and D.J.G.Ives, “the structural properties of alcohol-water mixtures,” *Q. Rev.*, vol. 20, pp. 1–44, 1966.

[48] R. Hoogenboom, H. M. L. Thijs, D. Wouters, S. Hoeppener, and U. S. Schubert, “Tuning solution polymer properties by binary water–ethanolsolvent mixtures,” *Soft Matter*, vol. 4, no. 1, pp. 103–107, 2008.

[49] W. Schartl, *light scattering from polymer solutions and nanoparticle dispersions*. springer, 2007.

[50] E. M. Seftel *et al.*, “LDH and TiO2/LDH-type nanocomposite systems: A systematic study on structural characteristics,” *Microporous Mesoporous Mater.*, vol. 203, no. C, pp. 208–215,

2015.

[51] H. Schnablegger and Y. Singh, “SAXS analysis,” in *The SAXS Guide*, 3rd ed., Anton Paar GmbH, 2011, pp. 1–99.

[52] X. Liu, Y. Zhao, X. Fan, and E. Chen, “Crystal orientation and melting behavior of poly(ε-Caprolactone) under one-dimensionally ‘hard’ confined microenvironment,” *Chinese J. Polym. Sci.*, vol. 31, no. 6, pp. 946–958, 2013.

[53] I. Teraoka, “Models of Polymer Chains,” in *Polymer Solution*, vol. 3, John Wiley & Sons, 2002, pp. 108–139.

[54] W. J. Lin, H. K. Lee, and D. M. Wang, “The influence of plasticizers on the release of theophylline from microporous-controlled tablets,” *J. Control. Release*, vol. 99, no. 3, pp. 415–421, 2004.

Acknowledgement

I would like to thank my supervisor, Alessandro Ianiro, for the patient guidance, encouragement and advice he has provided throughout my time as his student. I have been extremely lucky to have a supervisor who guided me through this complex system, and who responded to my questions so patiently. I have been motivated and inspired a lot from his attitudes towards work and the professional knowledge. By working side by side for 9 months, we became good friends rather than simply remained the relation between the supervisor and the student. I really appreciate to have this chance working with you and I wish you a very good lucky for your phD project and future life.

I must express my gratitude to my supervisor, Catarina Esteves, for her consistently support and useful advice during my project. I really expected and enjoyed every meeting I had with her, from her valuable guidance I can always find the tools that I needed to choose the right direction and successfully complete my project. Thanks for providing me such an interesting project and letting me be a member of SPC group. Also many thanks for the helps of finding the internship at Corbion.

I would like to thank Prof. Remco Tuinier for the warm welcome from SPC group, where I met many nice colleagues and had chance to work with them. I also would like to thank Heiner Friedrich to be my defense committee member and to provide valuable assessments for my thesis.

To those people who I met and who provided me with kindly helps during my project, I would like to also express my sincere thanks. Thank Macro for the patient and endless help for the large amount of SAXS measurements. Thank Ton for all the support I need throughout my project. Thank Alvaro for the theoretical support. Thank Laura for the use of DSC measurements. Thank Isabel for the help of my synthesis. Thank Pleunie for arranging the activities and everything I need during my time in SPC. Thank everyone in my office for the accompanies as well as all the SPC members. I will always cherish the time and memories I had in SPC.